AN EVALUATION OF HYDROSTRATIGRAPHIC CHARACTERIZATION METHODS BASED ON WELL LOGS FOR GROUNDWATER MODELING OF THE HIGH PLAINS AQUIFER IN SOUTHWEST KANSAS

By

Sarah R. Kreitzer

B.S., University of Tennessee at Chattanooga, 2008

Submitted to the Department of Geology and the Faculty of the Graduate School of the University of Kansas in partial fulfillment of the requirements for the degree of Master of Science.

P. Allen Macfarlane, Chairperson

J.F. Devlin

Leigh Stearns

Date Defended: March 28, 2011

The Thesis Committee for Sarah R. Kreitzer

certifies that this is the approved version of the following thesis:

AN EVALUATION OF HYDROSTRATIGRAPHIC CHARACTERIZATION METHODS BASED ON WELL LOGS FOR GROUNDWATER MODELING OF THE HIGH PLAINS AQUIFER IN SOUTHWEST KANSAS

P. Allen Macfarlane

Date approved: April 26, 2011

Abstract

The Ogallala portion of the High Plains aquifer is the primary source of water for irrigation and municipal purposes in southwestern Kansas. The spatial variability and connectivity of permeable and non-permeable deposits influence local ground-water flow and availability. The complex distribution of lithology, as well as the limited quality and quantity of high-resolution data sources, present challenges for subsurface characterization. This study uses conditional rules based on regional hydrogeologic knowledge, and a relational well log database of over 4,000 carefully-screened drilling logs to consistently translate sediment descriptions into a form useful for 2D and 3D characterization of the High Plains aquifer framework. Methods used to approximate the spatial distribution of hydrogeologic units differ in function, application, computational requirements, and the amount and type of information needed. Semivariograms and transition probability geostatistics show that low permeability units are laterally extensive, and can be spatially correlated at distances up to 1 km across the study area. The modeling work described in this report incorporates various spatial approximations of hydraulic parameters to demonstrate the influence of heterogeneity on the ground-water flow system. The results of this study contribute to the conceptual understanding of local heterogeneity in the hydrostratigraphic framework.

Acknowledgements

I would like to thank my advisor Dr. Allen Macfarlane for his encouragement, guidance, and support throughout my studies and in this research project. I thank my thesis committee, Dr. Rick Devlin and Dr. Leigh Stearns, for their time, suggestions, and comments. Geoff Bohling and Guisheng Li offered helpful guidance, discussions, assistance, and insightful comments. In addition, I thank Brownie Wilson for his help with data acquisition and information management, and Mark Schoneweis for figure preparation and editing. I greatly appreciate and am thankful to all individuals involved to make this study a success.

Table of Contents

List of Figures

List of Tables

Appendix

1.0 Statement of Problem

In response to water-level declines across the High Plains region, state and local agencies are assessing local water availability and formulating tailored management plans based on aquifer subunit delineation (Wilson et al., 2002). However, the limited availability of high-resolution data sources and the complex distribution of permeable and non-permeable deposits within the aquifer present challenges for accurate subsurface characterization. Although semi-continuous hydrostratigraphic units in the Ogallala Formation have been correlated over short distances, drill cuttings do not provide sufficient information to distinguish the units across the region (McLaughlin, 1946; Gutentag, 1963; Fader at al., 1964; Macfarlane and Wilson, 2006).

A geologic process-imitating model, which accounts for the physical mechanisms by which the sequence was deposited, would produce the best possible estimate of aquifer heterogeneity (Koltermann and Gorelick, 1996). Although incomplete knowledge of the geological processes affecting the region during the Neogene period make this an unlikely goal, it may be possible to approximate spatial characteristics of the hydrostratigraphic framework using a data-based approach. By mining and interpreting the information contained in carefully-screened drilling logs, aquifer characteristics can be estimated and used with additional data for local and regional subsurface investigations (Macfarlane and Schneider, 2007; Macfarlane, 2009). In a similar attempt to utilize existing data from drilling logs, Seni (1980) used lithologic descriptions from water well logs to map lithofacies of the Ogallala Formation in Texas. Dutton et al. (2001) demonstrated the regional continuity of permeable units using information obtained from drilling log descriptions. More recently, Macfarlane (2009) used a database of over 3,000 drilling logs to generate 3D visualizations of local variability in the distribution of permeable units within the saturated portion of the High Plains aquifer in southwestern Kansas.

1.1 Water Management Issues

The High Plains aquifer supplies approximately 30% of all U.S. irrigation water, and is the principal source of groundwater for southwestern Kansas (Sophocleous, 2005). As in other regions of western Kansas, ground-water levels across much of Southwest Kansas Groundwater Management District No. 3 (GMD3) are declining due to an imbalance between recharge rates and water-use (Gutentag et al., 1984; Wilson, 2007; Macfarlane, 2009; McGuire, 2009). Saturated thickness (ST), defined as the total thickness of saturated sediment between the water table and base of the aquifer, is used as a measure of ground-water availability in unconfined aquifers. In the past 60 years, ST has decreased by more than 40 % as water levels have declined up to 61 m in parts of the aquifer (Young et al., 2005; Macfarlane and Wilson, 2006). Based on average annual measurements by the Kansas Geological Survey (KGS), water levels have declined over 9 m in the past 10 years across parts of Stanton, Grant and Stevens counties.

To reduce the rate of water-level decline and conserve ground-water resources in southwest Kansas, the GMD3 rules and regulations (2004) establish minimum well spacing requirements in unconfined and confined areas of the aquifer and set criteria for the closure of townships to new groundwater appropriations. For instance, a township may be closed to further allocation if the average saturated thickness of the aquifer within the township is 15 m or less. In Kansas, the Kansas Water Appropriation Law protects senior water rights from direct, well-to-well impairment resulting from water diversion by junior water rights (KSDA, 2004). Updated regulations for impairment claims and investigations became effective October 29, 2010. The revisions set procedures for addressing impairment issues related to regional water-level declines.

1.2 Hydrostratigraphic Issues

The High Plains aquifer is a regionally unconfined aquifer that consists mainly of unconsolidated to cemented deposits of clay, silt, sand, and gravel. Measures of saturated thickness (ST) assume that all saturated deposits contribute water to pumping wells equally. However, fine-grained sediments like clay and silt, as well as locally cemented zones, form low permeability units that impede ground-water flow (Gutentag et al., 1981; Macfarlane and Wilson, 2006; Macfarlane, 2009). In southwest Kansas, unconsolidated sand and gravel deposits form semi-continuous preferential pathways for lateral and vertical ground-water movement. To provide a more accurate depiction of local ground-water availability in the region, the practical saturated thickness (PST) concept takes into account only the net thickness of saturated sediments that can transmit significant amounts of water to extraction wells (Macfarlane et al., 2005).

1.3 Purpose of the Study

The main objective of this study is to find the most effective method for translating material descriptions from over 4,000 drilling logs into a form useful for hydrostratigraphic characterization in the High Plains aquifer of southwestern Kansas (Figure 1.31). Additional objectives of this investigation include (1) comparison between KGS sample logs and drilling logs, (2) hydrostratigraphic characterization based on the information contained in drilling logs, and (3) development of hydraulic property maps for incorporation in a ground-water flow simulation. Simulation in this research is used only as an interpretive measure to evaluate the relative importance of lithologic complexity and connectivity in the local High Plains aquifer flow system.

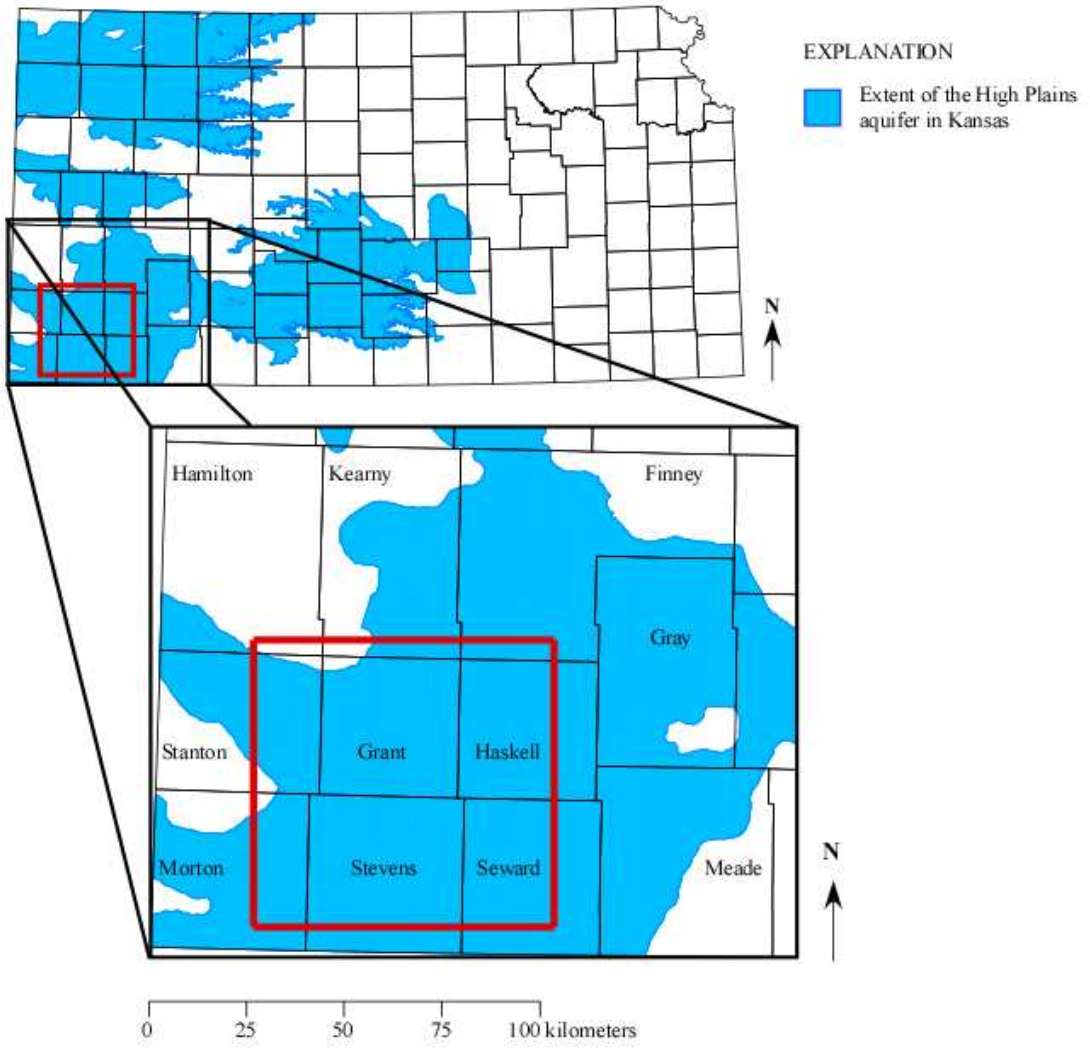

Figure 1.31. The study area (outlined in red) and extent of the High Plains aquifer in Kansas.

The first part of the thesis describes the setting of the study area in southwest Kansas, and includes an overview of regional hydrostratigraphic units and their corresponding hydraulic properties. The second portion of the thesis discusses various data-based methods used to translate descriptions from drilling logs into a form useful for characterizing the spatial distribution and interconnectivity of permeable units within the aquifer. The 2D and 3D approximations of subsurface variability provide the basis for a local ground-water flow simulation. Model results demonstrate the effectiveness of different methodologies in representing the spatial distribution of lithology for predevelopment conditions in the High Plains aquifer of southwestern Kansas.

1.4 Previous Work

In an early investigation of the High Plains region, Darton (1920) described the geology and ground-water resources of southern Hamilton and Kearny counties in a report that includes maps of geology, land surface topography, and water table depths. A few years later, Bass (1926) described the geology in Hamilton County and published a structural map of the Dakota Formation western Kansas. Smith (1940) assessed the Neogene geology of southwestern Kansas, and Latta (1941) reported on the ground-water resources in Stanton County in a bulletin published by the State Geological Survey of Kansas. In a later study, McLaughlin (1946) described ground-water conditions in Grant, Haskell, and Stevens counties.

Frye and Leonard (1952) conducted a study of the Pleistocene geology and described the Pleistocene drainage patterns in southwestern Kansas. Merriam and Frye (1954) investigated the Cenozoic sequence of western Kansas and constructed a map of the areal surface geology and topography of the bedrock surface underlying the Cenozoic deposits. The USGS published

annual water-level measurements in water-supply papers until 1956, when the State Geological Survey of Kansas commenced reporting the data in annual bulletins. In 1958, the Kansas Water Resources Board conducted an initial review of water supply and availability in the region (KWRB, 1958). Fader et al. (1964) reported on the hydrogeology of the aquifer for Grant and Stanton counties. Gutentag et al. (1981) conducted a subregional hydrogeologic investigation of the High Plains aquifer in southwestern Kansas. In a later study, Gutentag et al. (1984) described the geohydrology and physical characteristics of the regional High Plains aquifer. As part of the USGS Regional Aquifer Systems Analysis (RASA) program, Stullken et al. (1985) simulated groundwater conditions in a report on the High Plains region in western Kansas. Luckey et al. (1986) produced digital simulations of ground-water flow in the aquifer, and Weeks et al. (1988) summarized results of the regional High Plains RASA study.

2.0 The Regional Setting

2.1 Location and Extent of Study Area

The research area is located in the High Plains region of southwest Kansas and includes Grant County and parts of Finney, Haskell, Hamilton, Kearny, Morton, Seward, Stanton, and Stevens counties in T. 26 S. through T. 32 S. and R. 34 W. to R. 40 W. The size of the project domain is 80 km x 76 km.

2.2 Physiography

The regional High Plains aquifer underlies approximately 450,600 km^2 of the High Plains region in the Great Plains physiographic province and 79,000 km^2 in the western third of Kansas (Fenneman, 1946). The region is characterized by primarily flat to gently rolling upland plains,

broad valleys, shallow depressions, and areas of extensive sand dunes that stretch along the southern side of the Arkansas River (Frye, 1946; Frye and Leonard, 1952; Fader et al., 1964).

Figure 2.21 is a contour map of land surface elevations obtained from Digital Elevation Models (DEMs) from the USGS National Elevation Dataset (NED). The land surface slopes to the east at approximately 3.8 m/km, and ranges in elevation from 1034 m in Morton County to 785 m in Seward County. Depression features in the southeastern part of the study area are the result of local subsidence associated with evaporite dissolution in underlying Permian bedrock units (Frye and Leonard, 1952; Gutentag et al., 1984; Macfarlane and Wilson, 2006).

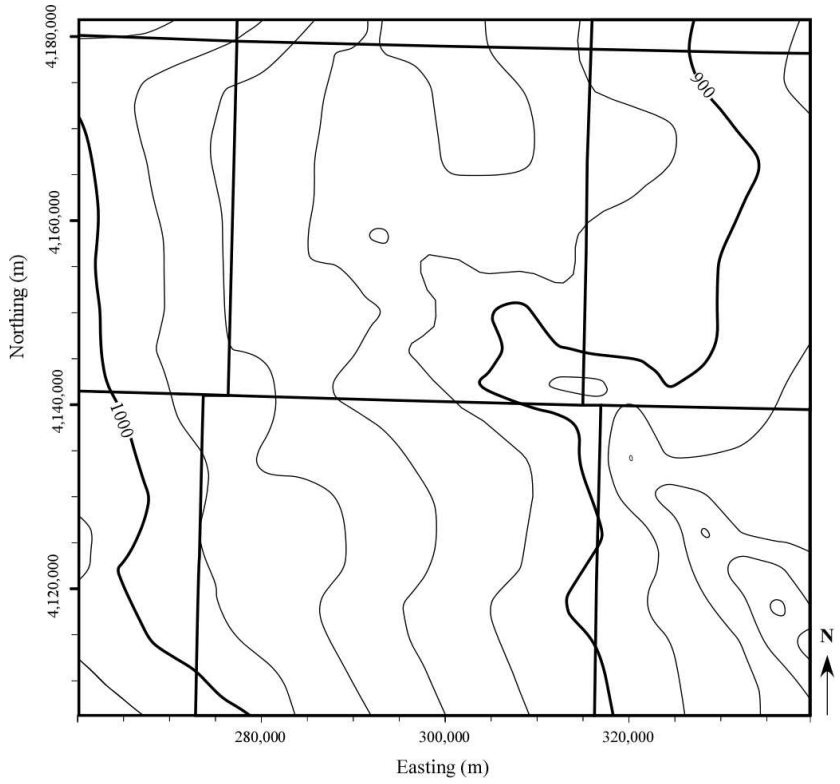

Figure 2.21. Generalized land-surface topography in the study area. Contour intervals are 20 m.

2.3 Climate

The High Plains region in southwestern Kansas is classified as a semiarid environment with low precipitation, high rates of evaporation, and frequent wind. Based on data extracted from the High Plains section-level database (Young et al., 2003), mean annual rainfall ranges from 38 cm in the west to 50 cm in the east, with approximately 75% of the annual precipitation occurring between April and October (Gutentag et al., 1981). The mean annual precipitation for 1961-1990 is 49 cm at the Garden City airport. Seasonal weather patterns are variable, with mean temperatures ranging from -1° C to 1° C in January and from 26° C to 28° C in July (Dugan and Peckenpaugh, 1985). Evapotranspiration rates increase during the summer months, and precipitation is greatest during the spring (Long et al., 2003).

2.4 Drainage

The Cimarron River flows in an arc-shaped path through southwest Kansas and is intermittent in Grant, Stevens, and Morton counties (Whittemore et al., 2005). During predevelopment, the water table surface was shallow along the Cimarron river valley in Kansas, and small streams flowed south of Ulysses during wet periods (McLaughlin, 1946; Fader et al., 1964; Sophocleous, 2005; Young et al., 2005). Tributaries of the Cimarron River include the North Fork branch of the Cimarron River, Sandy Arroyo Creek, and Lakin Draw. Sandy Arroyo Creek merges with the North Fork branch in western Grant County, and the two forks of the Cimarron converge in southeastern Grant County. In southern Grant County, bluffs along the river valley rise 37 to 55 m above the floodplain and are incised by numerous deep, short draws. The Cimarron River flows out of Grant County at an elevation of 860 m (Fader et al., 1964).

Predevelopment water depths in the study area range from the land surface to more than 120 m below land surface, with a mean water depth of 72 m. The predevelopment water table elevation ranges from 783 m in the east to 988 m in the west. The shape and slope of the water table determine the rate and direction of ground-water flow. Irregularities in the water table configuration are often the result of (1) bedrock surface topography, (2) discharge of groundwater into streams, (3) recharge of the aquifer by ephemeral streams, (4) irregular contributions of water to the aquifer, (5) local variations in transmissivity, and (6) pumping of water from wells (McLaughlin, 1946). As indicated by the downstream flexures in the water table map (Figure 2.41), the Cimarron River is a losing stream in northwestern Stevens County, southeastern Grant County, and southwestern Haskell County. Downstream flexures of water table contours near Bear Creek in northwestern Grant County signify water seepage through the stream bed into the aquifer (McLaughlin, 1946). Upstream flexures of water table contours along the Cimarron River in southwestern Grant County suggest discharge of groundwater to the Cimarron River and the North Fork tributary.

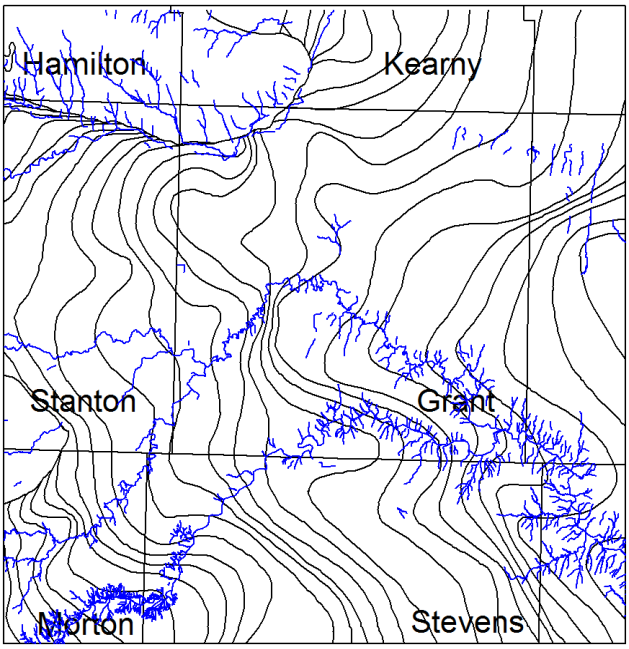

Figure 2.41. Predevelopment water table contours and drainage patterns (modified from Young et al., 2005).

2.5 Geologic Structure

In southwest Kansas, deeply-incised Permian and Cretaceous bedrock units dip to the east-northeast at 2.3 m/km with local relief as much as 28 m/km (Gutentag et al., 1981; Young et al., 2005; Macfarlane and Wilson, 2006). Dissolution and removal of bedded evaporites from underlying Permian bedrock units have modified the land and bedrock surfaces, and the regional geologic structure (Frye, 1950; Gutentag et al., 1981; Macfarlane and Wilson, 2006). Macfarlane and Wilson (2006) concluded that the Crooked Creek and Bear Creek faults in the northern part of the study area are discontinuous zones of dissolution characterized by related subsidence and small-scale faulting. Figure 2.51 presents contour maps of bedrock surface topography and Neogene sediment thickness based on a study by Macfarlane and Wilson (2006). Neogene sediment thickness, computed as the difference between the land surface and bedrock, ranges from approximately 12 m to 229 m in the study area, and is thickest in topographic lows within drainage channels or in regions affected by dissolution-related subsidence (Gutentag et al., 1980; Macfarlane and Wilson, 2006; Macfarlane, 2009). Bedrock elevation data for the GMD3 area are based on digitized contours of the bedrock surface (Macfarlane and Wilson, 2007).

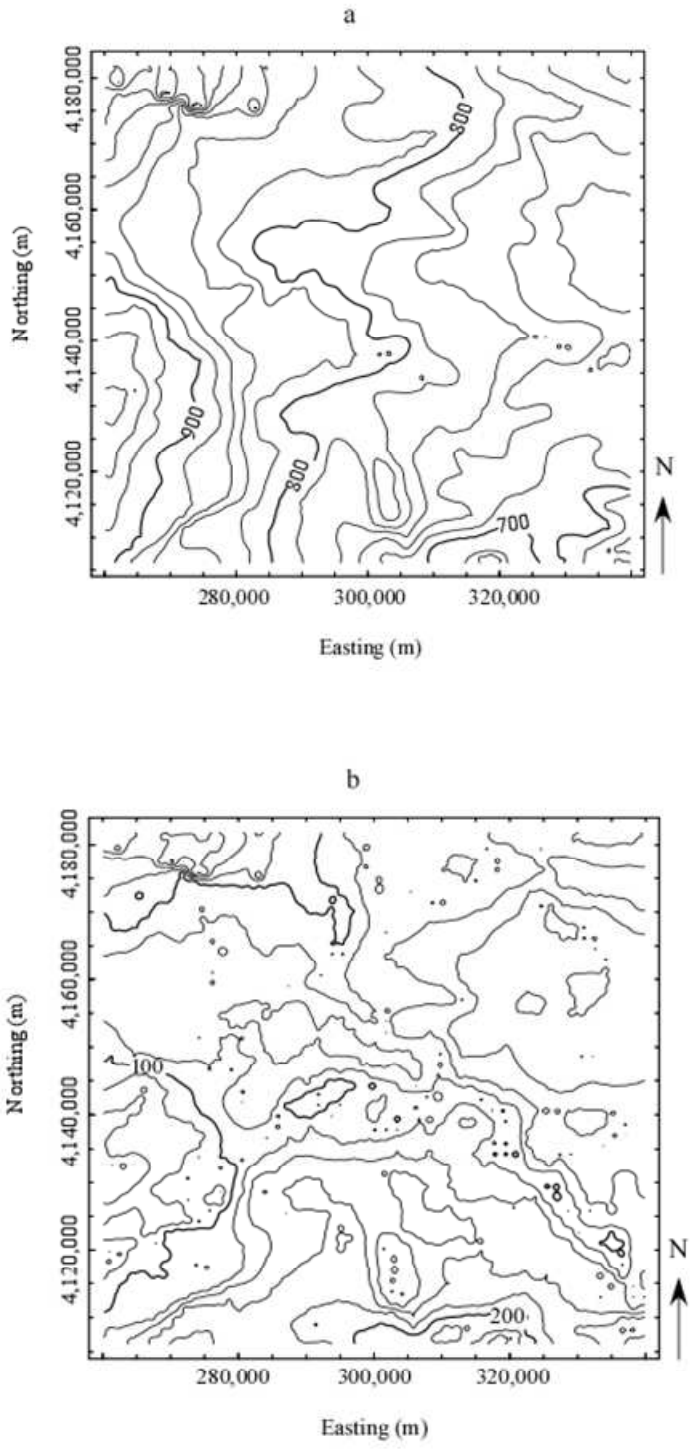

Figure 2.51. Contour maps of (a) bedrock surface topography and (b) Neogene sediment thickness (modified from Macfarlane and Wilson, 2006). The contour interval is 20 m.

2.6 Stratigraphy

The stratigraphic nomenclature of rock units in southwestern Kansas in relation to regional and local aquifers is summarized in Table 2.61 (Moore et al., 1951; Macfarlane, 2000; Ludvigson et al., 2009).

Table 2.61. Stratigraphic nomenclature in relation to regional and local aquifers (modified from Moore et al., 1951; Macfarlane, 2000; Ludvigson et al., 2009).

<table>
<tr><th>Era</th><th>Period</th><th colspan="2">Epoch</th><th colspan="2">Rock Stratigraphic Unit</th><th colspan="2">Aquifer</th></tr>
<tr><td rowspan="4">Cenozoic</td><td rowspan="4">Neogene</td><td rowspan="2">Quaternary</td><td>Holocene</td><td colspan="2">Alluvium</td><td colspan="2">Alluvial aquifer</td></tr>
<tr><td>Pleistocene</td><td colspan="2">Undifferentiated terrace, alluvial, and eolian deposits</td><td colspan="2" rowspan="3">High Plains aquifer</td></tr>
<tr><td colspan="2">Pliocene</td><td colspan="2" rowspan="2">Ogallala Formation</td></tr>
<tr><td colspan="2">Miocene</td></tr>
<tr><td rowspan="5">Mesozoic</td><td rowspan="5">Cretaceous</td><td colspan="2" rowspan="2">Upper</td><td rowspan="2">Colorado Group</td><td>Greenhorn Limestone</td><td colspan="2" rowspan="2">Upper Dakota confining unit</td></tr>
<tr><td>Graneros Shale</td></tr>
<tr><td colspan="2" rowspan="3">Lower</td><td colspan="2">Dakota Formation</td><td rowspan="3">Dakota aquifer</td><td>Upper Dakota aquifer</td></tr>
<tr><td colspan="2">Kiowa Formation</td><td>Lower Dakota confining unit</td></tr>
<tr><td colspan="2">Cheyenne Sandstone</td><td>Lower Dakota aquifer</td></tr>
</table>

Stratigraphic units in the High Plains region vary geographically, and are often differentiated on the basis of fossil assemblages, volcanic ash beds and lithology (Hibbard, 1953, 1958; Frye et al., 1956). The Pearlette ash bed, an important stratigraphic marker, is exposed in sec. 1, T. 30 S., R. 36 W. of Grant County, and is discontinuous across the study area (Fader et al., 1964). Gutentag (1964) used the Pearlette Ash bed to distinguish lower Pleistocene deposits, and subdivided Quaternary deposits in the Grant-Stanton area into Upper Pleistocene and Lower Pleistocene units composed of dominantly fine and coarse sediments, respectively. Fader et al. (1964) used fossil evidence to differentiate Lower Pleistocene deposits from the underlying Ogallala Formation in Grant County and eastern Stanton County, and distinguished the Pleistocene-Pliocene and the Upper-Lower Pleistocene boundaries in parts of southwestern Kansas using fossil mollusks. Previous studies have attributed limited success in consistently recognizing the boundary between Pleistocene and Pliocene deposits to a lack of stratigraphic markers and to the fact that the lithologic character of both units is similar (McLaughlin, 1946). Current research at the KGS involves the use of chemostratigraphic methods to show that a stratigraphic framework of the Cenozoic sequence can be constructed based on ash bed dating, paleontologic taxonomy, carbon content, and carbon isotope systematics (Macfarlane and Schneider, 2007).

2.7 Neogene Lithologies in the High Plains Sequence

Lithology, sediment thickness, and layer continuity are variable throughout the region. The High Plains aquifer framework in southwest Kansas is composed of a heterogeneous assemblage of Neogene gravel, silt, sand, clay, freshwater limestone, and marl. Sub-rounded to sub-angular gravel phenoclasts are composed of quartz, quartzite, gneiss, marble, granite,

orthoclase feldspar, basalt, metamorphic rocks, and reworked sandstone fragments derived from various sedimentary, igneous, and metamorphic sources. General fining-upward trends and less common coarsening-upward successions occur within the Neogene sequence. Upward-fining sequences of silt and fine sand are frequently overlain by thick deposits of relatively impermeable clay and silt. The effect of changes in lithology can be seen in the refraction of flow lines that occur at the boundary between adjacent hydrostratigraphic units of differing hydraulic conductivity (Domenico and Schwartz, 1990; Macfarlane, 1993).

2.8 Neogene Depositional History

The lithologic complexity and variability in depositional thickness and sedimentological character of the High Plains aquifer are attributed to cycles of erosion, deposition, and stability resulting from (1) Miocene-Pliocene episodes of uplift and erosion of the Rocky Mountains and Colorado Piedmont, (2) climate change, and (3) evaporite dissolution in underlying Permian bedrock units (Gutentag et al., 1984; Leonard, 2002; McMillan, 2002, 2006; Molnar, 2004; Pazzaglia and Hawley, 2004; Macfarlane and Wilson, 2006; Macfarlane and Schneider, 2007).

Near the end of the Miocene, regional uplift of the High Plains and Rocky Mountains subsequently increased stream gradients and incision of the High Plains surface (Gutentag et al., 1984). As streams aggraded and filled erosional valleys through the Pliocene, streams coalesced over former divides to form alluvial valleys. Coarse sand and gravel stream deposits occur in the lower section, with finer material deposited in small lakes and flood plains (Frye and Leonard, 1952). As the rate of uplift diminished during late Pliocene to early Quaternary time, fluvial deposition decreased and an extensive period of erosion ensued (Trimble, 1980; Macfarlane, 1993). During the early Pleistocene, streams incised the Pliocene surface with the greatest

incision rates occurring near the Front Range of the Rocky Mountains (Frye and Leonard, 1952). In late Pleistocene time, streams aggraded and deposited fine sand, silt, and gravel in fining-upward and coarsening-upward transitions (McLaughlin, 1946; Gutentag et al. 1984). Highly permeable sand and gravel deposits within coarsening-upward successions suggest high sediment transport capacity and a proximal sediment source, while upward-fining trends indicate a decrease in stream flow, transport capacity, or flow depth (Gustavson, 1996). As the climate became dryer and cooler during Quaternary time, erosion and eolian deposition became dominant.

3.0 The Hydrostratigraphic Units in the Study Area

Dakota Aquifer System

The Dakota Formation underlies the northern part of the study area in Grant County, northwestern Seward County, northern Morton County, and much of Finney, Kearny, Hamilton and Stanton counties. It is absent in much of Stevens and Seward counties, the southeastern corner of Haskell County, and a part of northern Stevens County (McLaughlin, 1946). As summarized in Table 2.61, major hydrostratigraphic units in the study area include the Lower Dakota aquifer, the Lower Dakota confining unit, the Upper Dakota aquifer, the Upper Dakota confining unit, the High Plains aquifer, and the overlying alluvial valley aquifers. The Lower Dakota aquifer consists of sandstone bodies in the Cheyenne Sandstone. In some areas, shale of the lower Dakota confining unit separates the Lower and Upper Dakota aquifers. The upper Dakota aquifer is composed primarily of mudstones, siltstones, and lenses of very fine to coarse-grained sandstones of the Dakota Formation in southwest Kansas. The geometric mean of

hydraulic conductivity for the Dakota aquifer in western Kansas is 6 m/d (Macfarlane et al., 1990).

Upper Dakota Confining Unit

In parts of the study area, the Dakota aquifer is separated from the overlying High Plains aquifer by the upper Dakota confining unit, a relatively impermeable sequence of chalk, shale, limestone, and siltstone (Macfarlane, 1997). The aquitard includes strata from the Graneros Shale and the Greenhorn Limestone (Table 2.61). In the northern portion of the study area, the Dakota Formation is hydraulically connected to the overlying High Plains and alluvial valley aquifers to form a single system (Kume and Spinazola, 1985; Macfarlane, 1993).

High Plains Aquifer

The High Plains aquifer in southwest Kansas is composed of saturated deposits of unconsolidated to cemented sand, silt, gravel and calcrete, including the Miocene-Pliocene Ogallala Formation and hydraulically-connected undifferentiated Pleistocene deposits (Gutentag et al., 1984). Semi-continuous deposits of highly permeable sand and gravel form preferential pathways for ground-water movement, while relatively impermeable deposits of silt, clay, and cemented material impede flow and act as local confining layers. Appendix A contains regional estimates of hydrogeologic properties published in previous ground-water studies.

Alluvial Valley Aquifers

Eolian deposits of fine loess and dune sand cover large areas of the High Plains region in southwest Kansas. Dune sands are shaped into hills and ridges by the wind, and are important

aquifer recharge zones. In most areas of southwest Kansas, the water table is below the dune sand (McLaughlin, 1946; Breyer, 1975; Gutentag et al., 1984).

3.1 Hydrogeologic Setting

During the predevelopment period, prior to large-scale irrigation development around 1950, the High Plains aquifer was in a state of relative equilibrium where recharge, on average, was equal to the amount of discharge. Sources of predevelopment recharge to the aquifer include underflow from the west and northwest, infiltration from precipitation, seepage from streams, and infiltration of groundwater from underlying bedrock units (Stullken et al., 1985; Sophocleous, 2005; Young et al., 2005). In a regional study, Luckey et al. (1986) estimated that annual recharge in the High Plains region ranged from 2.18 mm to 26.2 mm. Fader et al. (1964) estimated an average precipitation-recharge rate of 7.62 mm/yr across Grant and Stanton counties. Ground-water discharge from the High Plains aquifer occurs by means of evapotranspiration, subsurface flow to the east, and seepage to surface waters during wet seasons. Along the southern and eastern edges of the Syracuse anticline, water from the Dakota Formation moves southeastward into the Tertiary and Quaternary deposits of Grant County (McLaughlin, 1946).

Hydraulic conductivity and specific yield are related to sediment characteristics, and vary both vertically and laterally across the region. Using lithologic descriptions and representative values of hydraulic conductivity, Gutentag et al. (1981) estimated an arithmetic mean hydraulic conductivity of 24.3 m/d in southwestern Kansas, and reported an average flow velocity of about 0.3 m/d. Hydraulic conductivity values from aquifer tests performed in the region are presented in Appendix A, and range from 7.60 to 30.5 m/d, with a mean of 24.7 m/d (Fader et al., 1964;

Gutentag et al., 1984; Watts, 1985). Specific yield (S_y) ranges from approximately 0.004 to 0.30 in the High Plains aquifer (Young et al., 2003).

4.0 Methodology

This chapter describes the methods of data collection, compilation, interpretation, application, and analysis. General information about aquifer characteristics and water budget information are available from the KGS High Plains Aquifer Section-Level database (Young et al., 2003). Geographic locations, land surface elevations, and descriptions of lithology from 4,031 drilling logs in the study area are archived in the relational database. The log locations in the database use the North American Datum of 1927 (NAD 27). Using the conversion tool in RockWorks (RockWare, 2009), the coordinates are converted to the North American Datum of 1983 (NAD 83) for spatial interpolation and ground-water modeling. Figure 4.01 is a generalized flow chart of the methods used in the study.

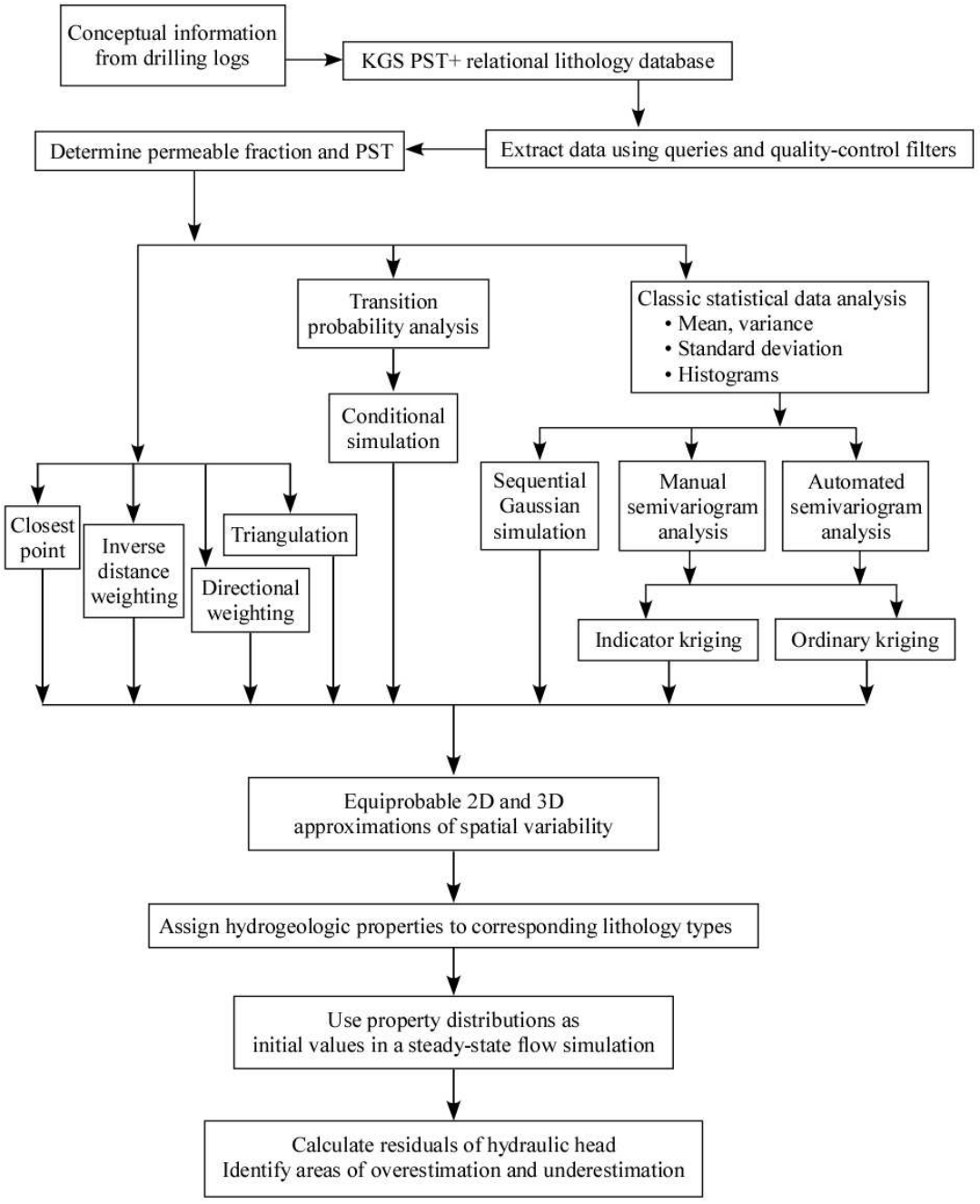

Figure 4.01. Generalized flow chart of methods used in the study.

4.1 Relational Lithology Database

An extensive lithologic database, developed in Microsoft Access as part of the KGS Practical Saturated Thickness Plus (PST+) program, contains original, unaltered lithologic descriptions from (1) water well completion (WWC-5) records submitted to the Kansas Department of Health and Environment (KDHE) and archived at the KGS since 1975, (2) sample logs produced by KGS scientists, and (3) logs from closely-spaced test holes drilled by contractors to find an optimal location for installing a high-productivity pumping well. Figure 4.11 is a location map of over 4,000 drilling logs extracted from the database for the study area.

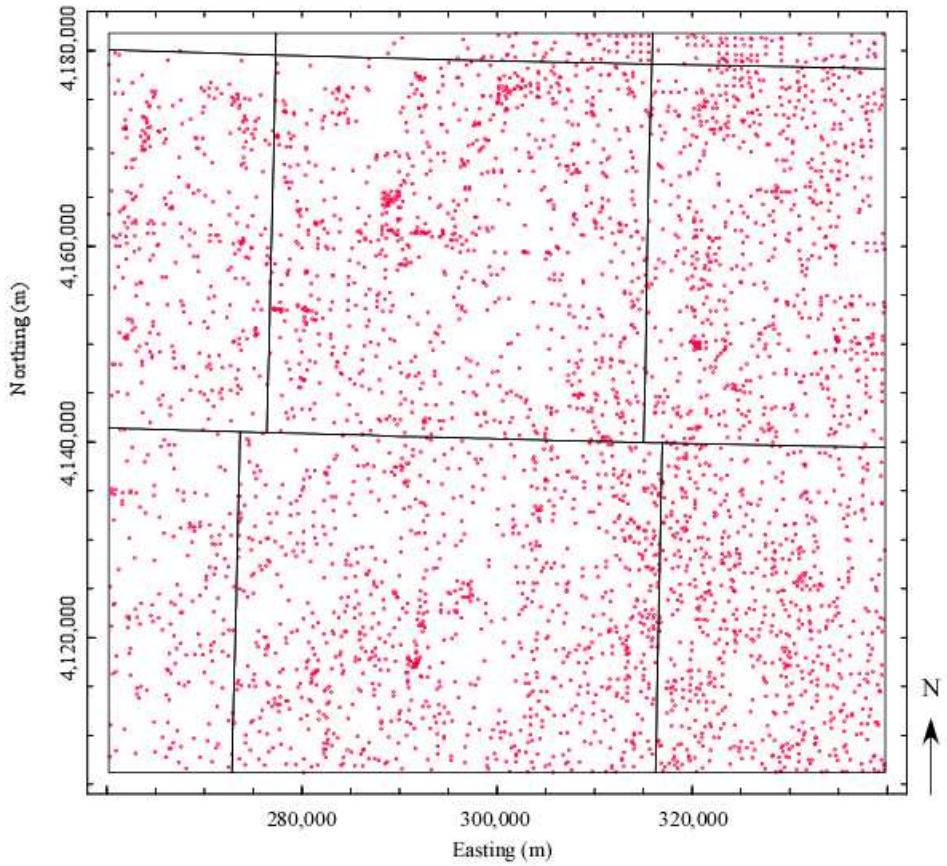

Figure 4.11. Location map of drilling logs used in the study.

The quality of information sourced from the database is highly variable, and must be filtered to ensure data quality control. To meet this objective, a criteria-based filter generates subsets of data based on the inclusion or exclusion of certain drilling contractors, certain lithologic terms, and the designated level of detail expressed as the average interval thickness per log entry. Figure 4.12 illustrates the database structure and layout.

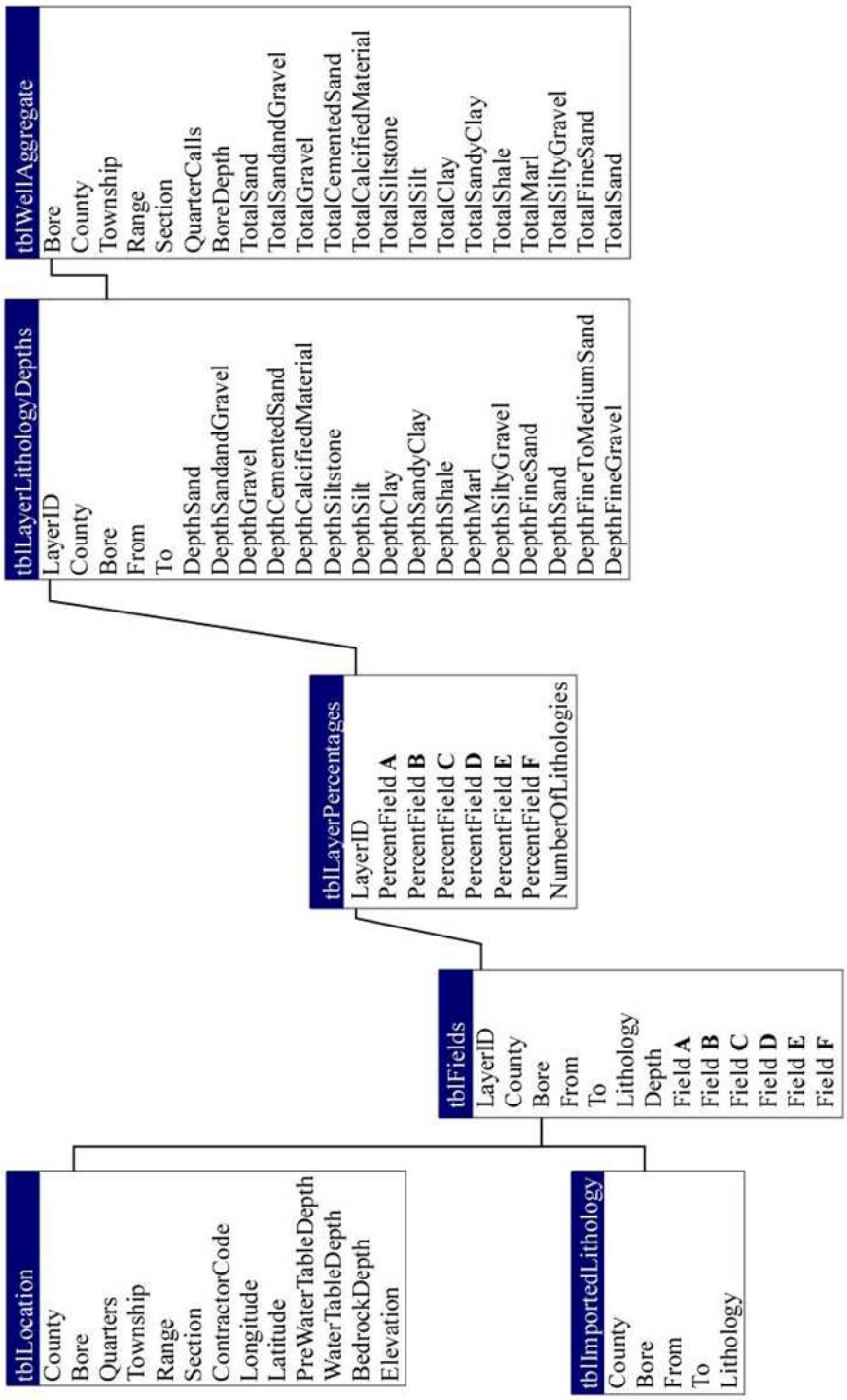

Figure 4.12. Relational file structure for archival and analysis of drilling log data.

Within the database, filtering tables are used to translate descriptions of lithology into a form useful for data analysis and parameter estimation. Table 4.11 is an example of the default table used to assign lithology fields to materials identified in each log entry, or layer. Appendix B contains the terms assigned to lithology types identified in the relational database, along with their associated regional hydrogeologic properties. The relative proportion of each sediment type in a layer is determined by user-defined rules in the database. Using the rules in Table 4.12, the layer described by "AstreaksB" is composed of 80% clay and 20% sand.

Table 4.11. Default fields table.

LayerID	Bore	From (m)	To (m)	Lithology	Phrase	FieldA	FieldB
416885	39551	1	13	Sandy clay and silt	AandB	sdc	s
416886	39551	13	24	Clay	A	c	
416887	39551	24	33	Sand w/ clay streaks	AstreaksB	snd	c

Table 4.12. Example percentage table used to estimate the proportion of each lithology type in a deposit.

Phrase	FieldA	FieldB	FieldC	Total
AandB	0.6	0.4	-	1.0
A	1.0	-	-	1.0
AstreaksB	0.8	0.2	-	1.0
ABC	0.5	0.3	0.2	1.0

4.2 Relative Permeability and Calculation of PST

In this investigation, conditional rules for quantifying the proportion of permeable material in each deposit are based on the concept of relative permeability, previous work and geologic knowledge, field and laboratory examination of drill cuttings, and comparison of drilling logs with KGS county bulletin and sample logs. The permeable fraction, which ranges from zero to one, generally corresponds to the relative permeability of different materials. Highly permeable materials like unconsolidated sand and gravel transmit significant quantities of water through the aquifer, and have a permeable fraction of 1. Conversely, fine-grained deposits of clay and silt have a permeable fraction of 0. The permeable fraction values assigned to each lithology type are listed in Appendix B. Figure 4.21 illustrates the concept of relative permeable fraction encountered at depth within the aquifer. In a layer containing multiple sediment types, the mean permeable fraction is calculated as a weighted average based on relative abundance. The relative permeable thickness of individual layers is calculated as the product of mean permeable fraction of layer thickness. The predevelopment practical saturated thickness (PST), a measure of ground-water availability, is computed the sum of all relative permeable thickness estimates for the interval between the predevelopment water table and the bedrock surface.

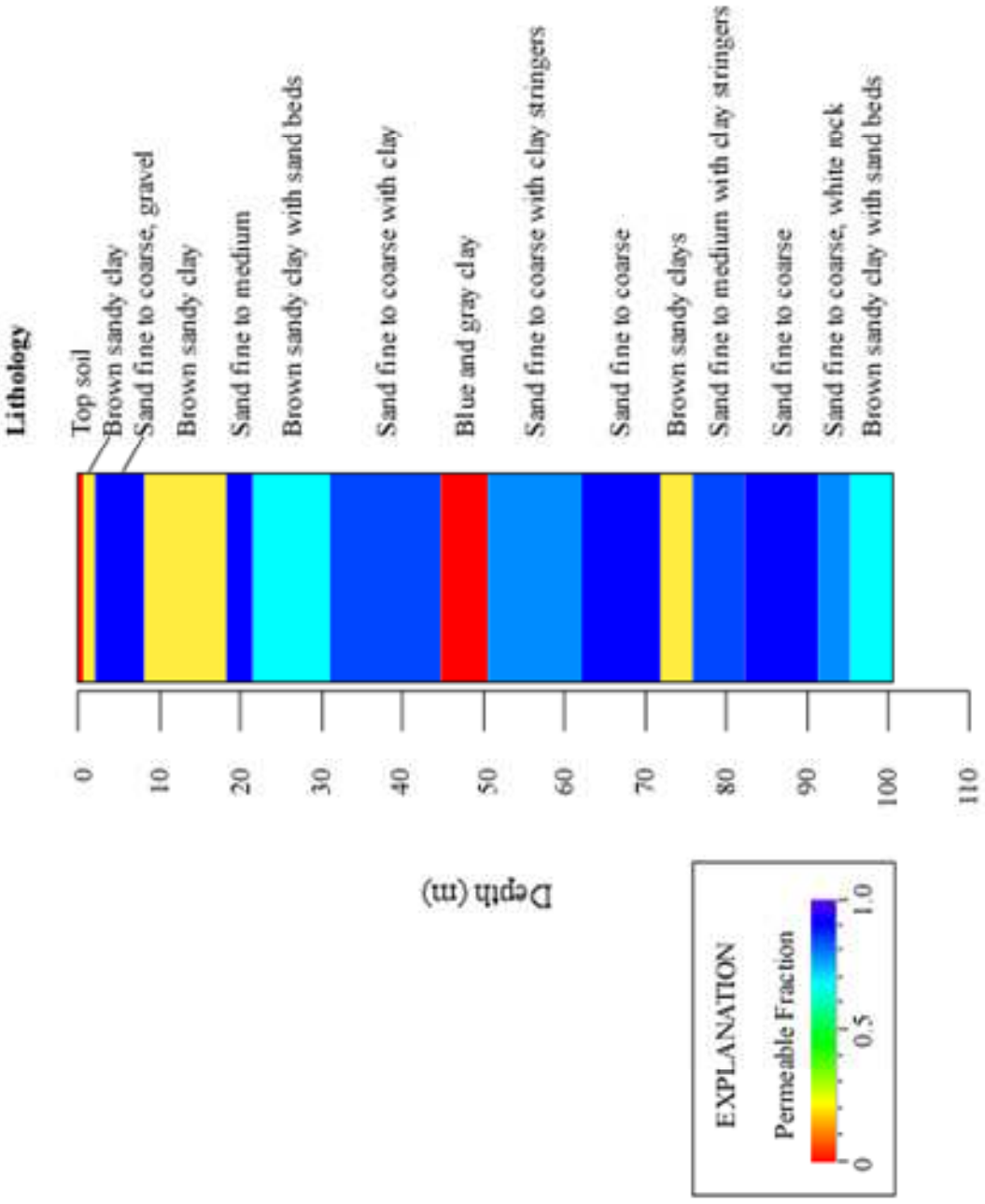

Figure 4.21. Vertical profile of the permeable sediment fraction.

4.3 Discretization of the High Plains Aquifer

Spatial discretization of the study area is necessary to represent the spatial distribution of hydraulic parameters in a numerical model. The region is discretized into 200 East/West rows of nodes and 190 North/South columns of nodes with a uniform spacing of 400 m. Based on the average minimum distance between data points, a horizontal node spacing of 400 m allows for spatial characterization at the scale of a quarter-section. The declustering program in RockWorks reduces the bias imposed by clustered sample data by assigning the average of all points in a 400 m^2 grid cell to the center of the cell block. To visualize the vertical distribution of lithology, the 3D solid model diagram generated in RockWorks 14 uses a vertical spacing of 10 m and 55 vertical nodes for a total of 2,030,994 voxels. As illustrated in Figure 4.31, each voxel is a 3D cell defined by the x, y, and z location coordinates of its node. A fourth parameter assigned to the voxel represents the value of an associated hydrogeologic variable, and can be used to estimate unknown values at neighboring locations.

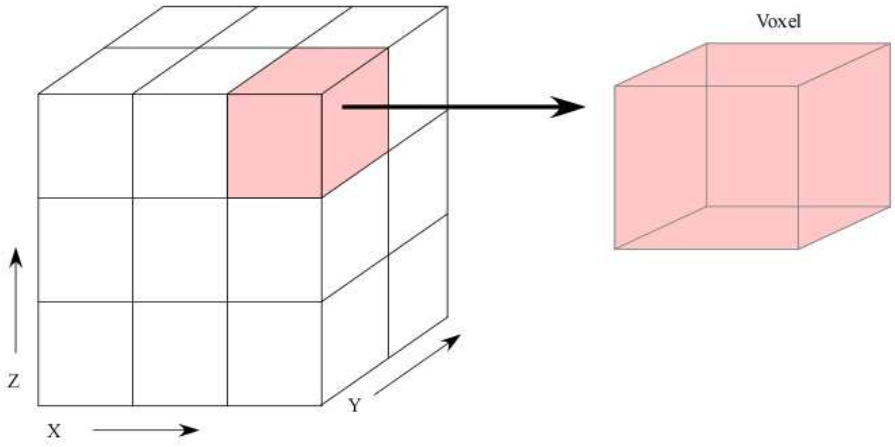

Figure 4.31. A 3D voxel grid and cell.

4.4 Characterization Methods

In this study, the methods that incorporate drilling log data for hydrostratigraphic characterization vary in application, complexity, and effectiveness. The data-based methods used in this study to construct 2D and 3D visualizations of permeable fraction and PST include (1) closest point, (2) triangulation, (3) inverse distance weighting, (4) directional weighting, (5) kriging, (6) sequential Gaussian simulation (SGS), and (7) transition probability-based geostatistics (Deutsch and Journel, 1992). Koltermann and Gorelick (1996) and de Marsily et al. (2005) review various geostatistical methods used to represent the spatial distribution of sediment types. Various kriging techniques are described in detail by Isaaks and Srivastava (1989) and Deutsch and Journel (1992). Computer programs used for spatial characterization include (1) RockWorks 14, (2) TPROGS, (3) WinGSLIB, (4) SGEMS, and (5) the R statistical program GSTAT.

The RockWorks (RockWare, 2009) program offers a variety of simple gridding and interpolation techniques, including closest point, triangulation, inverse distance weighting, and directional weighting. The closest point algorithm assigns the value of the nearest data control point to unknown grid nodes without regard to separation distance or direction. This method is commonly used for spatial interpolation due to its simplicity and minimal computational requirements. Triangulation is a grid-based approach that uses a network of triangles to determine unknown grid values. The inverse distance method incorporates anisotropy by assigning a weighted average of neighboring data points to unknown values. Directional weighting uses the inverse-distance method with a directional weighting bias.

To account for spatial variability in the data, this study uses various 2D and 3D kriging routines in RockWorks and GSLIB to represent the spatial structure and characteristics of local

variability, and account for (1) the proximity of data to the unknown location, (2) clustered and irregularly-spaced data, and (3) the structural continuity of the simulated variable. The accuracy of kriged estimates depends on the kriged parameter, data density, and the semivariogram model used to describe the spatial structure. A semivariogram model curve fit to the empirical data in a trend-free direction is assumed to represent the spatial interdependence in the data (Kitanidis, 1997; Olea and Davis, 2003; Bohling and Wilson, 2005).

In Figure 4.41, the semivariogram plots the variance of paired PST values as a function of lag, or separation distance. The increase in semivariogram values from the origin to the sill corresponds to a decrease in correlation with increasing separation distance (Isaaks and Srivastava, 1989). The semivariogram components include the nugget, sill, range, and lag. The nugget effect represents discontinuity at the origin due to measurement error and small-scale variability. If the semivariogram value is greater than 0 at the origin, then this value is referred to as the nugget. The sill represents the variance of the data, and the range is the distance at which the semivariogram model reaches the sill. Data pairs at distances greater than the range are considered uncorrelated (Bohling, 2005). Bohling (2005) reviews additional geostatistical methods and discusses details of the semivariogram analysis.

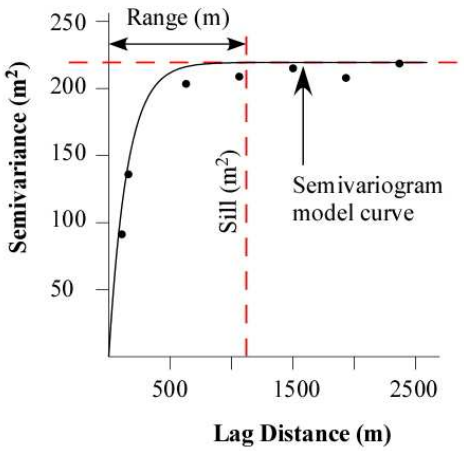

Figure 4.41. Semivariogram components.

The best-fit semivariogram model is selected based on visual inspection of the empirical semivariogram, as well as semivariogram-fitting techniques implemented in the R statistical software package GSTAT (Pebesma and Wesseling, 1998). Using the model parameters as input for ordinary kriging equations, the GSLIB 2D kriging program (KB2D) generates parameter grids and corresponding maps of prediction uncertainty. In addition to kriging, the best-fit semivariogram model parameters are incorporated in a sequential Gaussian simulation (SGS) to generate multiple, equiprobable approximations of PST that honor existing data and reproduce the input histogram and semivariogram.

A more sophisticated approach for characterizing the geometry and spatial continuity hydrostratigraphic involves the use of transition probability-based geostatistics (Deutsch and Journel, 1992). To approximate the spatial connectivity and proportion of lithologic units in the study area, the transition probability approach accounts for observable characteristics of categorical data that include volumetric proportions, mean lengths, juxtapositional tendencies, and anisotropy, and spatial variations (Carle, 1998; 1999). Different types of sediment identified

in the log descriptions are assigned to four indicator variables based on values of permeable fraction. The indicator variables describe the presence or absence of a particular lithology at a certain location, *x*. An indicator variable $I_k(x)$ can be defined by

$$I_k(x) = \begin{Bmatrix} 1, \textit{ if category } k \textit{ is present at } x \\ 0, \textit{ otherwise} \end{Bmatrix},$$

where *k* represents a class of lithology (Carle, 1999). Transition probability in one dimension is expressed as:

$$t_{jk}(h) = \Pr(k \text{ occurs at } x + h \mid j \text{ occurs at } x),$$

where and *j* and *k* represent different sediment types. The transition probability between indicator variables *j* and *k* for lag *h* is the probability that *k* occurs at location $x + h$ given that category *j* occurs at *x* (de Marsily et al., 2005). Carle and Fogg (1996, 1997) describe the mathematical details of the transition probability approach. To illustrate the concept of transition probability, Figure 4.42 shows the vertically successive occurrences of 4 sediment categories. In Figure 4.43, the transition count matrix tallies the upward transitions from one category to another.

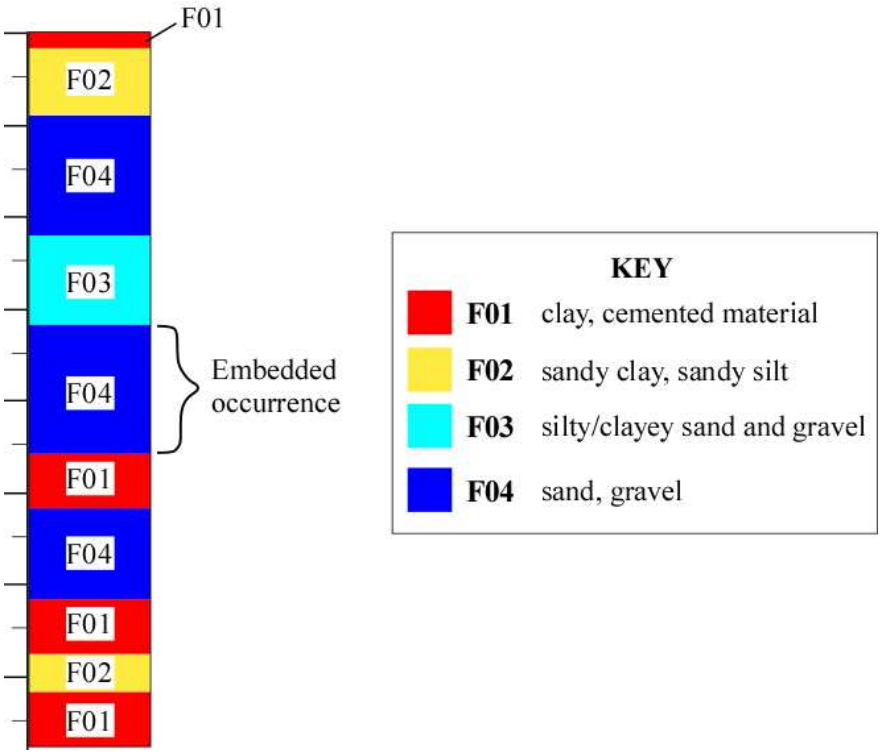

Figure 4.42. Diagram showing the embedded occurrences of four sediment categories.

	F01	F02	F03	F04
F01	0	2	0	1
F02	1	0	0	1
F03	0	0	0	1
F04	2	0	1	0

Figure 4.43. The transition count matrix for the vertical succession in Figure 4.42.

Diagonal elements in the transition count matrix are equal to zero because the embedded occurrence assumes that self-transitions between individual beds of similar lithology are indistinguishable. The transition probabilities are calculated by dividing the row values in the count matrix by the row sum. Based on the assumption that the juxtapositional tendencies and material proportions observed in the vertical direction also hold true in the horizontal directions, the T-PROGS 3D Markov chain modeling utility, MCMOD, uses the vertical Markov chain to generate a model of spatial variability for the *x* and *y* directions (Carle, 1996; Weissmann and Fogg, 1999; Weissmann et al., 1999; Jones et al., 2002). To incorporate asymmetry and juxtapositional tendencies in the data, Carle and Fogg (1996) suggest using transition probability diagrams in indicator kriging simulations of categorical data. Additional studies by Carle et al. (1998) and Fogg et al. (1998) use similar geostatistical techniques to estimate correlation lengths and the spatial distribution of aquifer parameters.

Criteria for assessing the uncertainty, strengths, and weaknesses associated with each characterization method include the relative ease of implementation, as well as the correlation between measured and estimated variables. Permeable fraction and PST residuals are calculated as the difference between the input and estimated data. The overall error is measured by the root mean squared (RMS) error, expressed as the square root of the mean sum of the square errors.

$$\text{RMS error} = \left[\left(\frac{1}{n}\right)\sum\left(h_m - h_s\right)^2\right]^{0.5}$$

The mean residual is the average difference between measured and simulated values, and the mean absolute error (MAE) is the average of the absolute residual values. The MAE is similar to RMS, but is less sensitive to large errors.

$$\text{MAE} = \left(\frac{1}{n}\right)\sum|h_m - h_s|$$

4.5 Groundwater Flow Modeling

Model Input

Data used for conceptual hydrogeologic characterization includes geologic contour maps, cross sections, drill cuttings, potentiometric surface maps, climate data, and hydraulic parameter maps available in published reports from the KGS and USGS (Luckey and Becker, 1999; Liu et al., 2010). This study used Visual MODFLOW Pro 4.3 to assess the influence of hydrogeologic conditions and aquifer heterogeneity on the ground-water flow system, calculate water budgets, and estimate water levels and flow directions. Developed by the USGS, MODFLOW is based on a finite-difference approximation of the governing ground-water flow equation (Harbaugh et al., 2000). The general form of the governing equation for ground-water flow, upon which the simulation was developed, is defined by:

$$\frac{\partial}{\partial x}\left(K_x\frac{\partial h}{\partial x}\right)+\frac{\partial}{\partial y}\left(K_y\frac{\partial h}{\partial y}\right)+\frac{\partial}{\partial z}\left(K_z\frac{\partial h}{\partial z}\right)+R=0$$

The directional components of hydraulic conductivity are represented by K_x, K_y, and K_z, and R is a source/sink term. The governing equation describes the steady-state flow of ground water through a heterogeneous and anisotropic porous medium (Anderson and Woessner, 1992).

Model Grid

Similar to the spatial discretization described in Section 4.3, the MODFLOW grid is composed of 200 East/West rows and 190 North/South columns. Based on the average minimum spacing between boreholes, uniform grid cells are 400 m by 400 m. In a regional study of the High Plains aquifer, Stullken et al. (1985) used a coarse grid of 4.57 km by 4.57 km cells to develop a steady-state flow simulation for predevelopment conditions. As part of the USGS Regional Aquifer Systems Analysis, Luckey et al. (1986) simulated both predevelopment and transient aquifer conditions for an area of approximately 244,000 km^2 in the northern High Plains region using uniform 16 km by 16 km grid cells. Luckey and Becker (1999) simulated predevelopment water levels in the central High Plains region using a finite-difference ground-water flow model with a grid cell size of 1.8 km x 1.8 km. As part of a recent KGS modeling project in the High Plains region of western Kansas, Liu et al. (2010) developed a calibrated transient model to simulate the flow system and stream-aquifer interactions using a uniform grid cell size of 1.6 km by 1.6 km.

Boundary Conditions

Boundary conditions define the hydrogeologic conditions at the model perimeter and are necessary to generate a unique solution to the flow equation (Anderson and Woessner, 1992). Boundary conditions are a source of uncertainty, especially if they do not correspond to the

natural physical boundaries of the aquifer (Watts, 1985). Inactive cells are assigned where the observed water level is at or below the bedrock surface to avoid numerical instabilities. Flow calculations are conducted only within the active cells. There are 37,137 active cells in the model, giving a total active model area of 14,855 km^2, about 98% of the model domain. The hydraulic boundary at the top of the model was initially assigned a constant rate of recharge, and was later modified during the sensitivity analysis. The boundary at the base of the model below the relatively impermeable bedrock layer is treated as a no-flow boundary. Constant head cells are assigned along the northern and southern boundaries of the domain. Drains are designed to allow groundwater to leave the aquifer system and simulate ephemeral stream conditions.

A general head boundary (GHB) simulates head-specified flux along the x-direction on the eastern and western boundaries of the domain. The GHB Package in MODFLOW calculates flow through the boundary (Q_b) as a linear function of the head difference between head at or outside the boundary and in the aquifer (h) (Anderson and Woessner, 1992). The conductance of the GHB is the product of average hydraulic conductivity and cell width, divided by the saturated thickness. Since the calibrated 2D regional model (Liu et al., 2010) does not provide information about the vertical variation of hydraulic head in the aquifer, the initial hydraulic head assigned along the model boundaries is considered to remain constant with depth. Figure 4.51 shows the model boundaries and active area of the project domain.

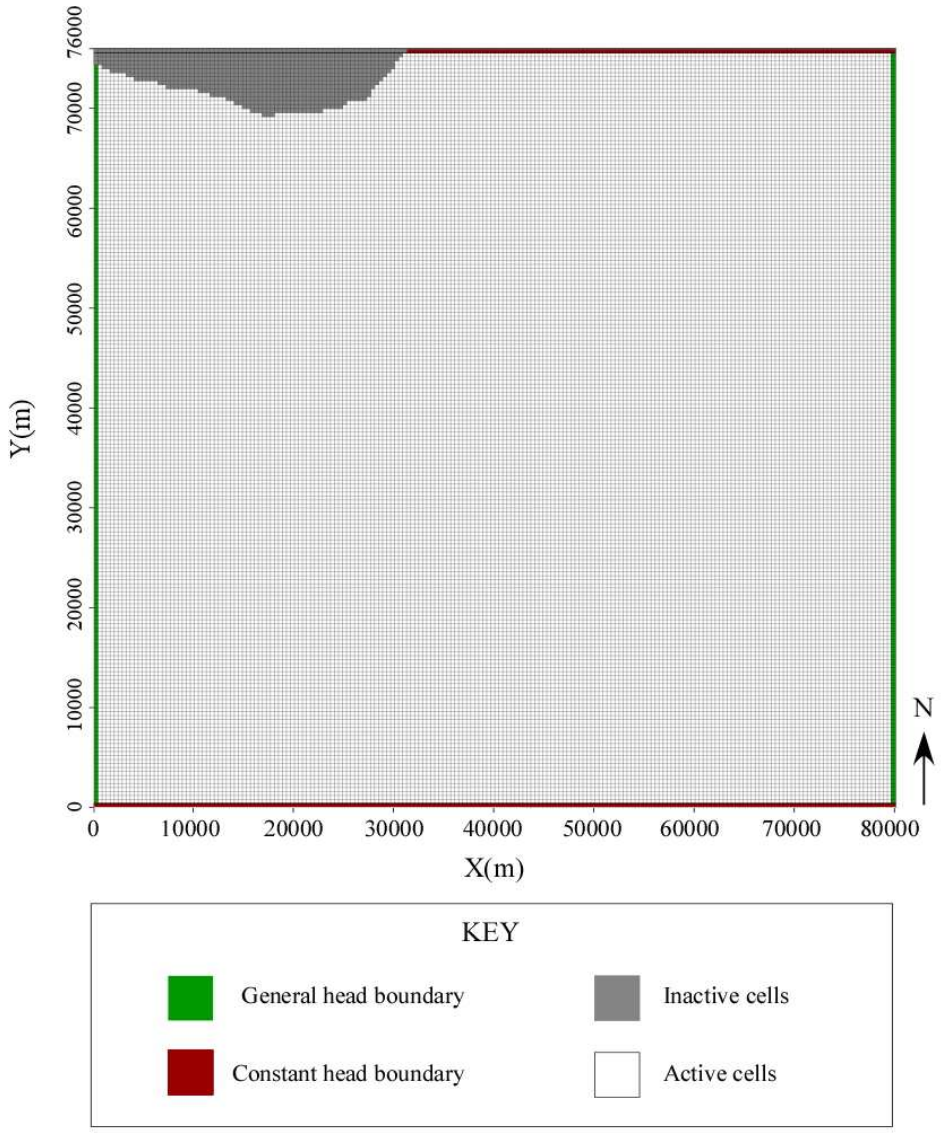

Figure 4.51. Model boundaries and active area of flow simulation.

Calibration

The parameter estimation program PEST (Doherty, 2004) facilitated the calibration of predevelopment ground-water conditions based on water-level measurements taken from 1929 to 1942 in 145 observation wells. These measurements and other relevant information are stored in the Water Information Retrieval and Storage Database (WIZARD) maintained by the Kansas Geological Survey (KGS). In addition, initial values of hydraulic head were estimated based on digitized water-level contours from the calibrated regional model (Liu et al., 2010). Figure 4.52 is a location map of predevelopment head observations used for model calibration.

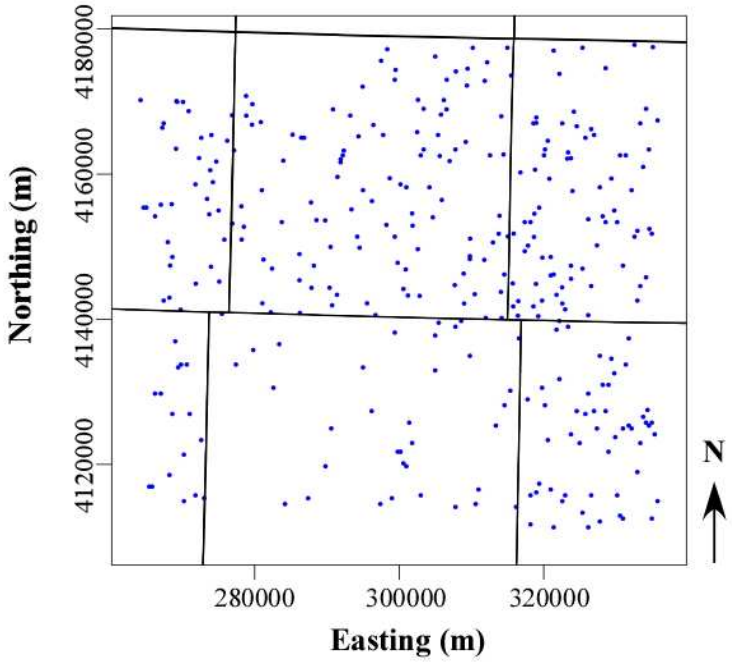

Figure 4.52. Predevelopment water-level observations used for model calibration.

Parameters adjusted during model calibration and sensitivity analysis include the conductance, boundary conditions, hydraulic conductivity, and weighting factors for different observation data. Calibration criteria for each simulation require (1) a general match between observed and simulated hydraulic heads, (2) a subregional water balance of approximately zero for predevelopment steady-state conditions, and (3) correspondence of simulated volumetric flow rates with the cell-by-cell flow rates of the calibrated regional model (Liu et al., 2010).

5.0 Results

This section presents a summary of predevelopment PST and permeable fraction, the results of field sampling, an overview of the relational lithology database, 2D and 3D visualizations, and the results of ground-water flow modeling.

5.1 Permeable Fraction and PST

Based on the relative proportion of permeable sediments in a deposit, the mean permeable fraction estimated from drilling log data in the project database ranges from 0 to 1.For descriptions containing multiple sediment types, the mean permeable fraction is calculated as a weighted average based on relative proportions. To assess the vertical distribution of permeable fraction, Figure 5.11 shows the mean permeable fraction averaged at depth intervals of 15 m within the study area. The vertical profile indicates that the mean permeable fraction is greatest between 823 m and 838 m, and lowest from 716 m to 732 m.

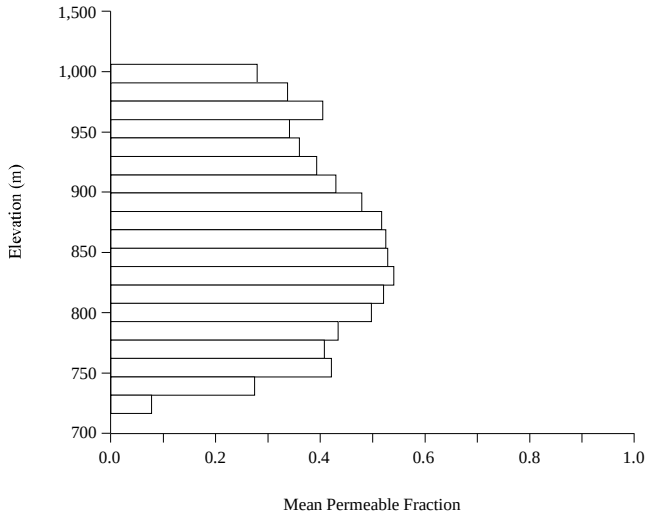

Figure 5.11. Permeable fraction averaged at vertical intervals of 15 m.

Figure 5.12 is a histogram of the vertically-averaged, predevelopment mean permeable fraction translated from 4031 drilling logs.

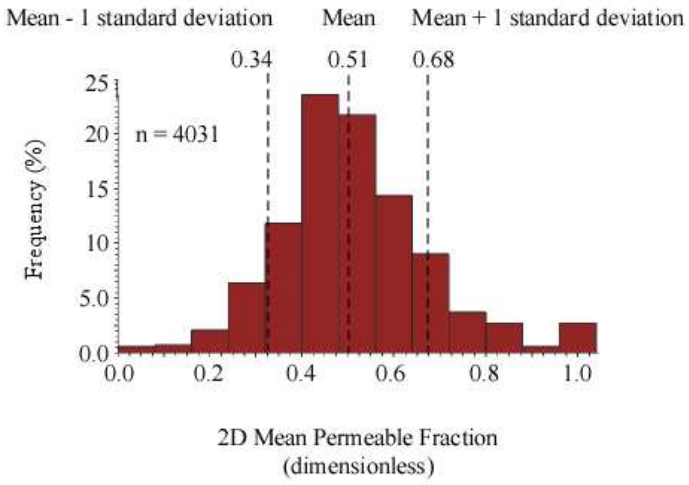

Figure 5.12. Histogram of depth-averaged predevelopment mean permeable fraction.

In Figure 5.12, the mean permeable fraction is distributed symmetrically about the mean, and is characterized by a mean of 0.51, a mode of 0.5, and a median value of 0.5. As discussed in Section 4.2, the practical saturated thickness (PST) accounts for only permeable deposits within the saturated interval. Based on estimates of relative permeability from 4031 drilling logs, the predevelopment PST in the study area ranges from 0 m to 143 m, with a mean of 42.8 m and a standard deviation of 21.2 m.

5.2 Field sampling

Field work in Finney, Haskell, Morton, and Seward counties conducted from May 2009 through July 2009 presented an opportunity to study sedimentary features observed in gravel pit exposures and outcrops, and to generate sample logs based on drill cuttings collected at depth intervals of 3 m for seven test holes drilled by Henkle Drilling and Supply Company, Inc. The location and lithologic descriptions from the test holes are presented in Appendix D. Sediment samples recovered from rotary drilling consist primarily of alternating sequences of unconsolidated to cemented sand, silt, clay, gravel, and small fragments of reworked local material. Mineralogically, sand grains are predominantly quartz with minor traces of mica, magnetite, pyrite, biotite, and orthoclase and microcline feldspar. Deposits of pedogenic carbonate, calcrete, and calcareous silt are observed throughout the sequence, and the most common cementing materials are calcium carbonate, iron oxide, and silica.

Drill cuttings recovered near the bedrock surface consist of yellowish-brown to reddish-brown ferruginous sandstone, siltstone, clay, and silty dark gray, reddish, and black shale. Sandstone fragments are identified as reworked material from the Dakota Formation. Deposits in the lower part of the Neogene sequence include fine- to coarse-grained sand and gravel, silt,

calcareous silt, variegated silty clay, and clay lenses. Sediment samples collected from test holes in Finney and Haskell counties grade upward into thin layers of mixed sand, small to medium-sized gravel clasts, and subordinate amount of silt. In Seward and Morton counties, lithology transitions upward into lesser amounts of coarse-grained sand and gravel mixed with unconsolidated clay and silt. Variably thick deposits of clayey silt, sandy clay, fine sand, and calcareous silt are present at depths of approximately 30 m in all test holes. To illustrate local spatial variations in lithology, Figure 5.21 shows a line profile diagram for relative permeability interpreted from three drilling logs in Finney County. Highly permeable units, in red, can be successfully correlated across the area between the three drill sites.

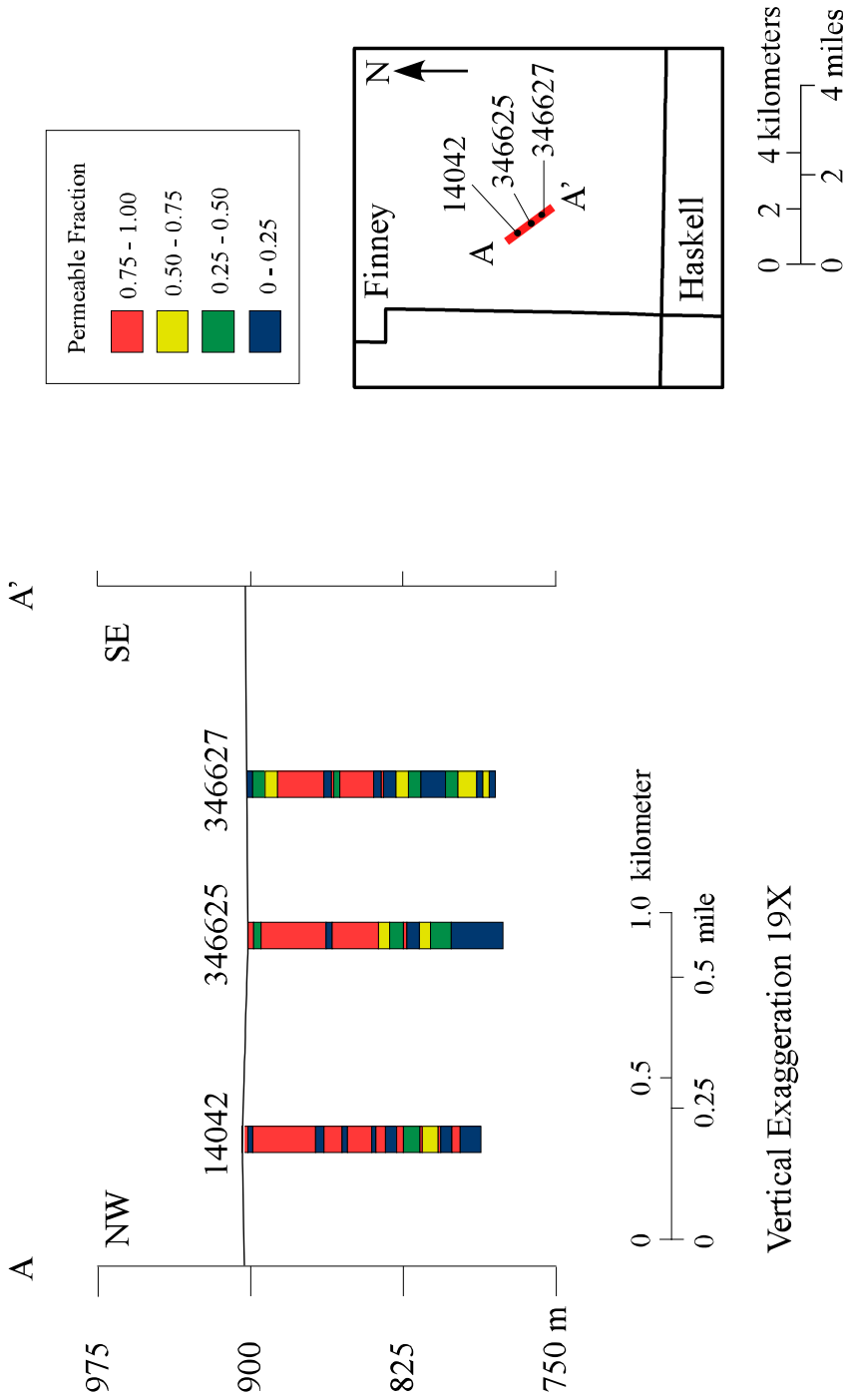

Figure 5.21. Line profile diagram A-A' shows the vertical distribution of permeable fraction in test-hole #346625, test-hole #346627, and one production well (#14042).

5.3 Database

Based on user-defined rules and methods of interpretation, the relational database can be used to consistently (1) translate material descriptions contained in drilling logs into lithologic terms, (2) quantify the relative contribution of each sediment type in the deposit based on the phrasing and order of material descriptions, and (3) estimate the proportion of the deposit thickness that is capable of storing and transmitting significant amounts of water to pumping wells. The database contains 66,070 individual layers containing descriptions of lithology from over 4,000 drilling logs in the study area. Of these observations, there are 37,254 descriptions of lithology within the predevelopment saturated interval. The average spatial density of drilling logs in the study area is approximately one log per 1.5 km^2, with an average separation distance of 484 m between boreholes.

A total of 70 terms are assigned to different types of lithology identified from drilling log descriptions. Appendix B lists each field, its associated lithology, relative permeability, and the frequency of each field within the saturated portion of the sequence. The material in 59% of the layers is described as a single field only, while multiple fields are used to describe materials in about 41% of the entries. The 1^{st} field is used for about 99% of the layers, the 2^{nd} for 41%, the 3^{rd} for 7.6%, the 4^{th} for 0.75%, the 5^{th} for 0.08%, the 6^{th} for 0.003%, leaving approximately 0.34% of all material fields null, or unknown. Approximately 28% of all reported materials are clay; clay exceeds all other descriptions by more than a 2:1 ratio. To ensure the veracity of drilling log data, quality control filters generate multiple data subsets from the original dataset based on user-defined criteria.

As discussed in Section 4.1, filtering criteria in the relational database are based on lithologic terminology, average interval thickness, and the drilling contractor. Within the

Neogene sequence, the average interval thickness is 11.4 m with a standard deviation of 8.16 m. Low interval thicknesses indicate greater detail in the logs. Elimination of drilling logs with an average interval thickness greater than three standard deviations from the mean (36 m) reduces the number of logs by 81, or approximately 2% of the original dataset. Filtering logs with an average interval thickness greater than 28 m, within two standard deviations of the mean, reduces the dataset by an additional 65 logs. Figure 5.31 is a histogram of the vertically-averaged, predevelopment mean permeable fraction calculated from the 3625 drilling logs with an average interval thickness between 3.3 m and 20 m, within one standard deviation of the mean (11 m). The quality control filters in the relational database reduce the number of logs and overall variance in the dataset. In Figure 5.31, the histogram of the filtered dataset is characterized by a lower standard deviation and variance than the original histogram of unfiltered logs (Figure 5.11).

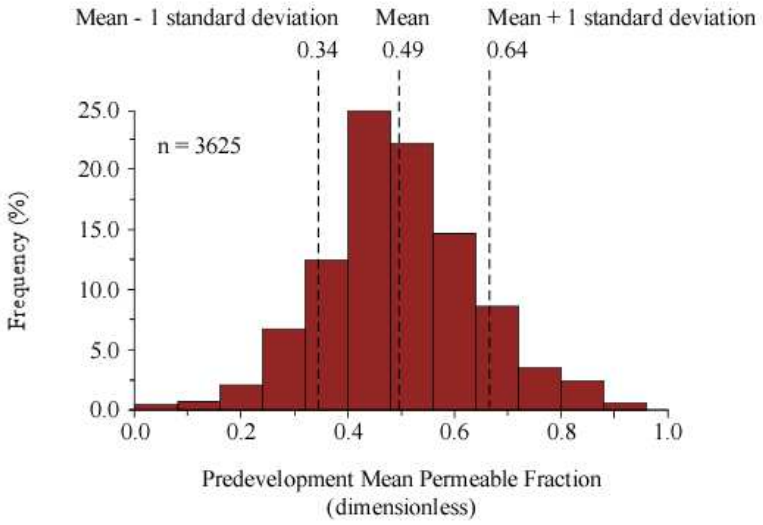

Figure 5.31. Histogram of depth-averaged, predevelopment mean permeable fraction based on 3625 drilling logs filtered from the database based on average interval thickness.

5.4 Characterization

In this study, various data-based methods used to generate grid-based maps from irregularly-spaced data include (1) closest point, (2) triangulation, (3) inverse distance weighting, (4) directional weighting, (5) kriging, (6) sequential Gaussian simulation (SGS), and (7) transition probability-based geostatistics (Deutsch and Journel, 1992). The methods vary in application, complexity, and effectiveness. The performance of each gridding or interpolation method is evaluated based on the magnitude and distribution of interpolation errors. In Appendix E, the residual error is calculated as the difference between observed and estimated values of PST. Low RMS errors indicate that the interpolation method is likely to give reliable estimates in regions of low data density. In Appendix E, the closest point algorithm with a high fidelity filter produced the highest correlation between estimated and observed PST values. The directional weighting approach implemented in RockWorks produced the highest RMS errors and lowest correlations between observed and simulated values. Figure 5.41 is a cross plot of observed and estimated PST based on the inverse distance weighting approach. Ideally, the estimate would be equal to the measured value and the cross plot would fall along a straight 45° line with a correlation of 1.

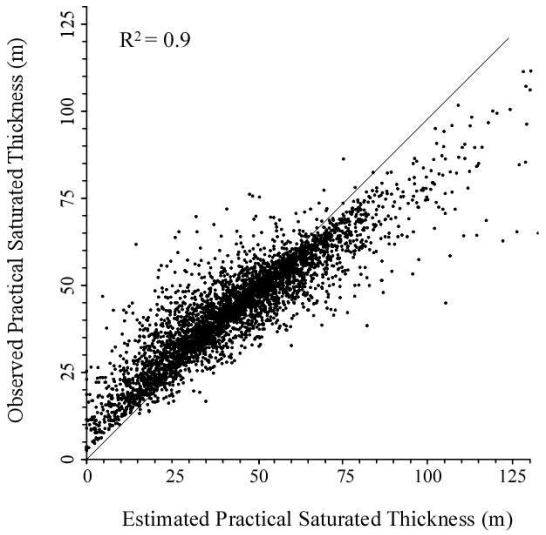

Figure 5.41. Cross plot of observed and estimated practical saturated thickness (PST) generated using inverse distance weighting in RockWorks 14.

Various methods of spatial characterization use semivariogram and transition probability models to represent the distribution and continuity of hydrostratigraphic units in the aquifer. As illustrated in Figure 4.41, the semivariogram components include the lag, range, and sill. Omnidirectional semivariograms assume that spatial correlation is the same in all directions, or isotropic (Bohling, 2005). To assess spatial anisotropy and estimate directions of maximum and minimum continuity, directional semivariograms are calculated using only pairs in the specified directions at horizontal lags of 400 m. Figure 5.42 shows the directional semivariograms of PST for the interval between the predevelopment water table and bedrock surface. Azimuth angles are given in degrees clockwise from north. The exponential semivariogram model fit to the empirical data along azimuths of 144° and 156°, measured clockwise from north, indicates that PST can be correlated with confidence at distances up to 1029 m in the study area. The best-fit model

parameters from the trend-free semivariogram in the direction N 36° E are used as input for kriging and sequential Gaussian simulation of PST.

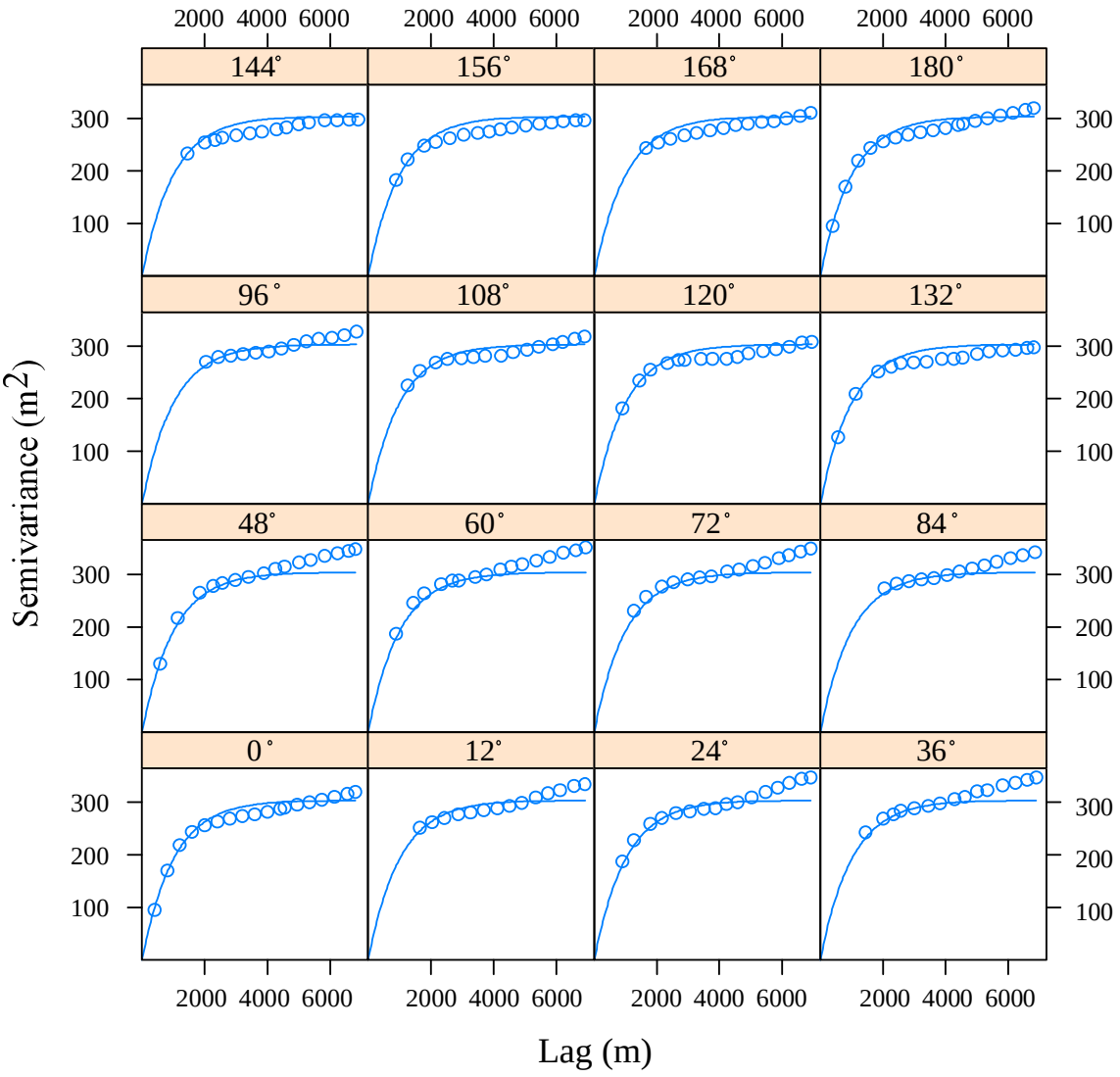

Figure 5.42. Measured points and modeled semivariogram curves for practical saturated thickness (PST) along azimuth angles in degrees clockwise from north.

Figure 5.43 is a grid-based map of PST generated in GSLIB using ordinary kriging with a trend using a search radius of 5000 m to estimate a local mean from surrounding data. Black dashed arrows along an azimuth of 144° correspond to the direction of the trend-free semivariogram model fit to PST in Figure 5.42. Greater PST along this feature may represent channel fill within a paleovalley (Macfarlane and Wilson, 2006).

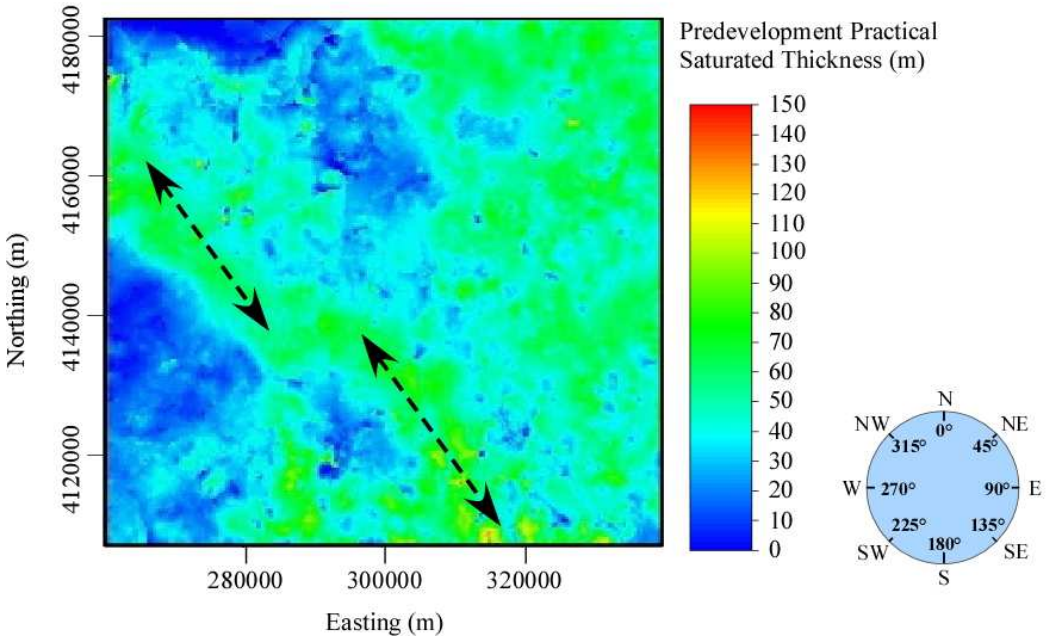

Figure 5.43. Map of PST generated using ordinary kriging with a linear drift, or trend, in both X and Y. Black arrows show trend a trend along an azimuth of 144°.

As outlined in Table 5.41, four classes of permeable fraction form the indicator variables used for the transition probability analysis and indicator kriging. For the purpose of this study, a permeable fraction of 0.6 separates high permeability sand and gravel from low permeability deposits of clay, silt, and cemented material.

Table 5.41. Designation and frequency of indicator variables in the study area.

Indicator	**Permeable fraction (*pf*)**	***n***	**Proportion (%)**	**Initial K (m/d)**	**Lithology**
F01	$pf = 0.00$	8717	31.02	0.1	clay, cemented sand, cemented sand and gravel, silt
F02	$0.00 < pf < 0.60$	10985	20.21	1.0	sandy clay, sandy silt
F03	$0.60 \leq pf < 1.00$	11833	12.92	10	silty or clayey sand, silty or clayey gravel
F04	$pf = 1.00$	9025	35.85	100	sand, sand and gravel, gravel

In Figure 5.44, the best-fit omnidirectional model for fine-grained deposits (F01) approaches a dimensionless sill of 0.01 at a horizontal range of 1212 m. The best-fit exponential semivariogram model for coarse-grained deposits (F04) approaches a sill of 0.01 at a horizontal range of 691 m.

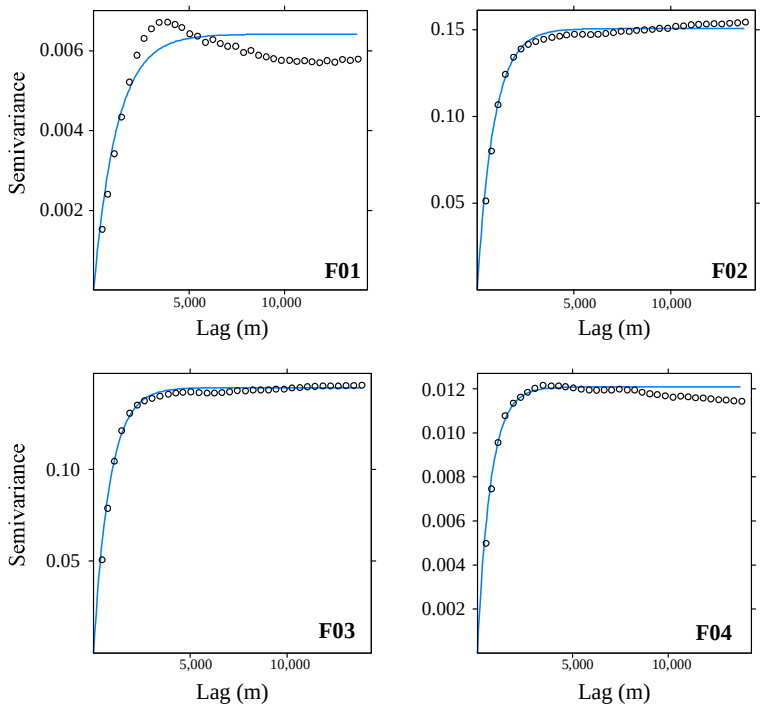

Figure 5.44. Empirical and model indicator semivariograms. The semivariance is dimensionless.

As summarized in Table 5.42, high permeability deposits of coarse unconsolidated sediment are the least laterally extensive class of sediment with the lowest range of the four indicator groups. Deposits of clay and cemented material are the most laterally extensive category of lithology. However, for intermediate sediment classes F02 and F03, the indicator semivariogram results are less conclusive. Similar range and sill values suggest that F02 and F03 could be combined to form three distinct lithology classes of lithology. For the purpose of this study, four indicator variables are used in the transition probability analysis to represent the spatial distribution and connectivity of sediment types.

Table 5.42. Best-fit omnidirectional semivariogram model parameters.

Indicator Variable	Semivariogram Model	Sill (dimensionless)	Range (m)
F01	Exponential	0.012	1212
F02	Exponential	0.15	870
F03	Exponential	0.14	837
F04	Exponential	0.006	691

Figure 5.45 compares the grids of mean permeable fraction generated using four different interpolation techniques. The ordinary kriging calculations use a maximum of 16 data points within a 5 km search radius to estimate the value of each unknown node. Ordinary kriging assumes that the mean is locally constant (Bohling, 2005b). In RockWorks, the default kriging algorithm incorporates an exponential semivariogram model with a nugget to characterize the spatial distribution of mean permeable fraction. The inverse distance weighting, triangulation, and default kriging approaches implemented in RockWorks use a single smoothing pass with a high fidelity filter to honor the input data. The high fidelity filter honors data points, while the smoothing pass reduces noise in the data (RockWare, 2009). Appendix E contains the residual errors of practical saturated thickness (PST) estimates generated from various gridding and interpolation techniques. Given the limited knowledge of local spatial variability in the aquifer, each random approximation of aquifer heterogeneity is equally likely. No single realization can be taken as a better representation of reality than another.

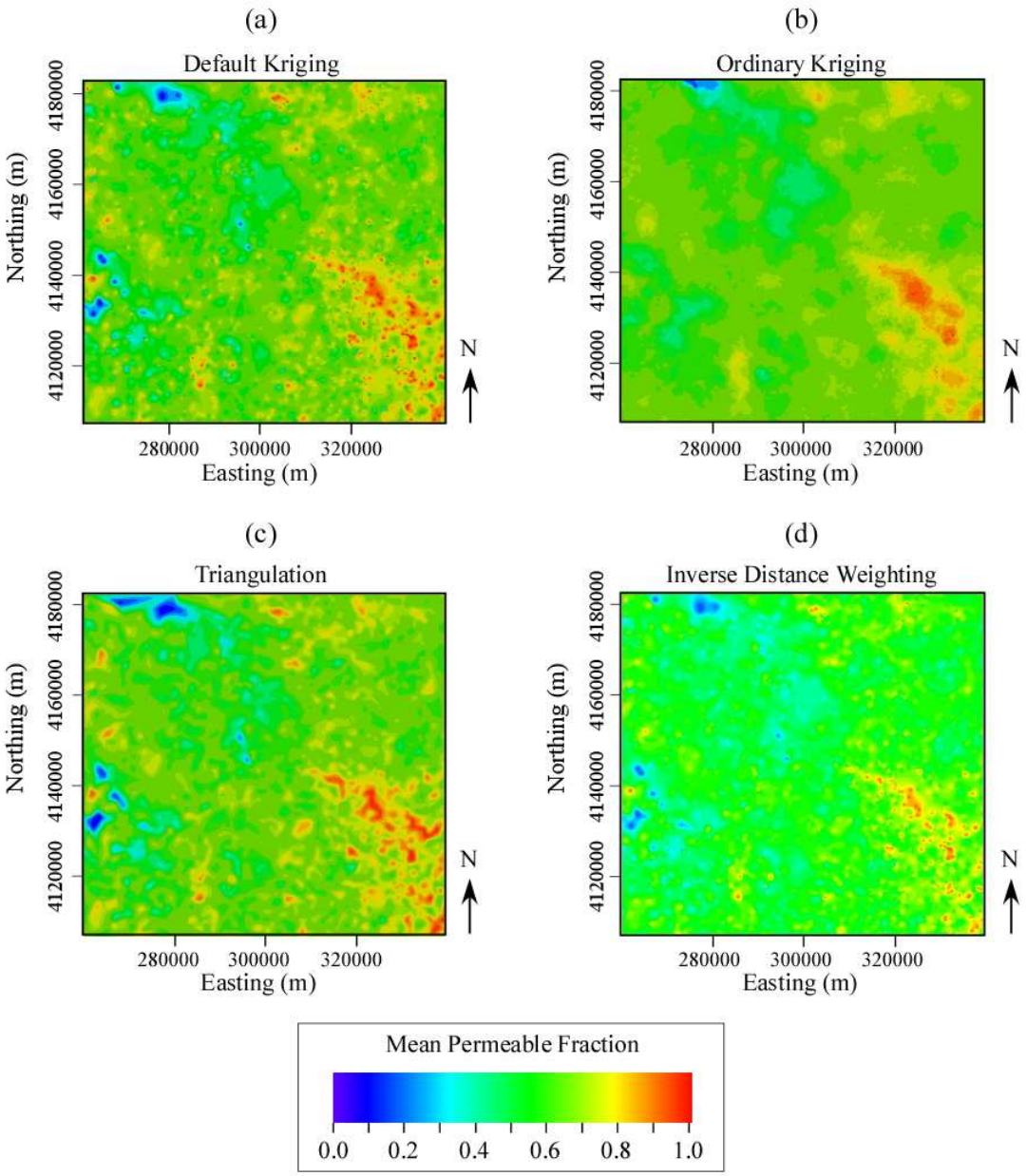

Figure 5.45. Grid-based maps of mean permeable fraction created using (a) the default kriging algorithm in RockWorks 14, (b) ordinary kriging in GSLIB, (c) triangulation, and (d) inverse distance weighting.

In this study, the transition probability-based geostatistical software (T-PROGS) uses Markov chains to model spatial variability in the distribution of permeable and non-permeable units that influence ground-water flow within the aquifer (Carle, 1999). Markov chains are fit to the transition probability measurements to estimate the mean length, or mean thickness, of each category within the vertical succession (Carle, 1999). In Figure 5.46, the solid lines represent Markov chain models fit to the vertical (*z*) direction transition probability measurements for indicator variables. The circles represent the transition probability measured from the drilling log data by the GAMEAS utility.

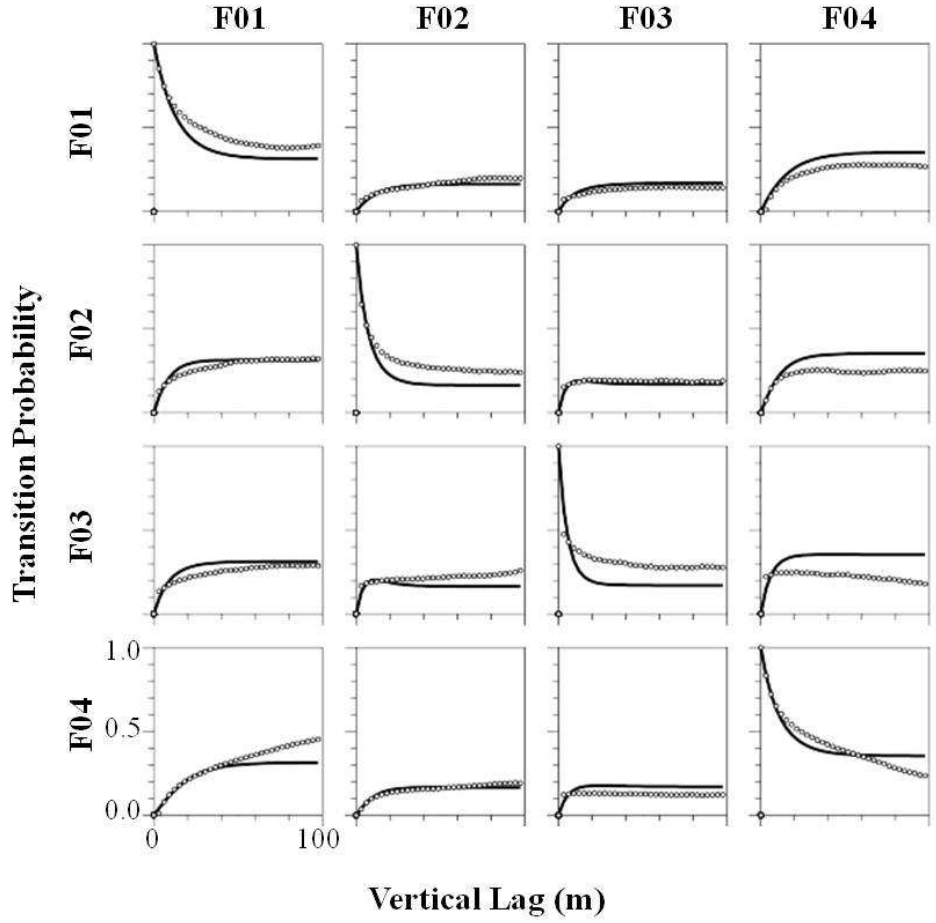

Figure 5.46. Measured transition probabilities (circles) and best-fit Markov chain models (solid lines) in the vertical direction.

Each of the plots contains two curves representing the vertical transition probability from one sediment type to another. As discussed in Section 4.4, the vertical model of transition probability is used to estimate the transition probability in the horizontal directions. The 3D Markov chain models are then used by the TPROGS utility TSIM as a basis for generating multiple approximations of spatial variability that honor existing data. Figure 5.47 shows one possible continuous representation of the indicator variables.

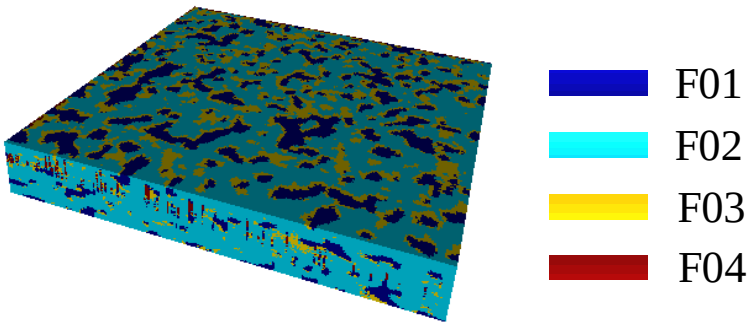

Figure 5.47. One possible distribution of indicator variables generated by TPROGS.

The solid model diagram generated in RockWorks is based on the closest point algorithm with a high fidelity filter. The 3D diagram can be viewed as cross sections, vertical profiles, or horizontal slices. Cross-sections illustrate the spatial variation in lithology across the study area, and are used to identify semi-continuous deposits of permeable material and local confining layers. Figure 5.48 is a cross-section (B-B') oriented northwest-southeast across the study area.

White dashes delineate the lateral connectivity of high-permeability zones. Figure 5.49 compares unsmoothed and smoothed fence diagrams of permeable fraction. The high fidelity filter is used in both diagrams to better honor the input data. The unsmoothed diagram shows a greater volume of low permeability deposits. The smoothed diagram exhibits greater spatial continuity of permeable units.

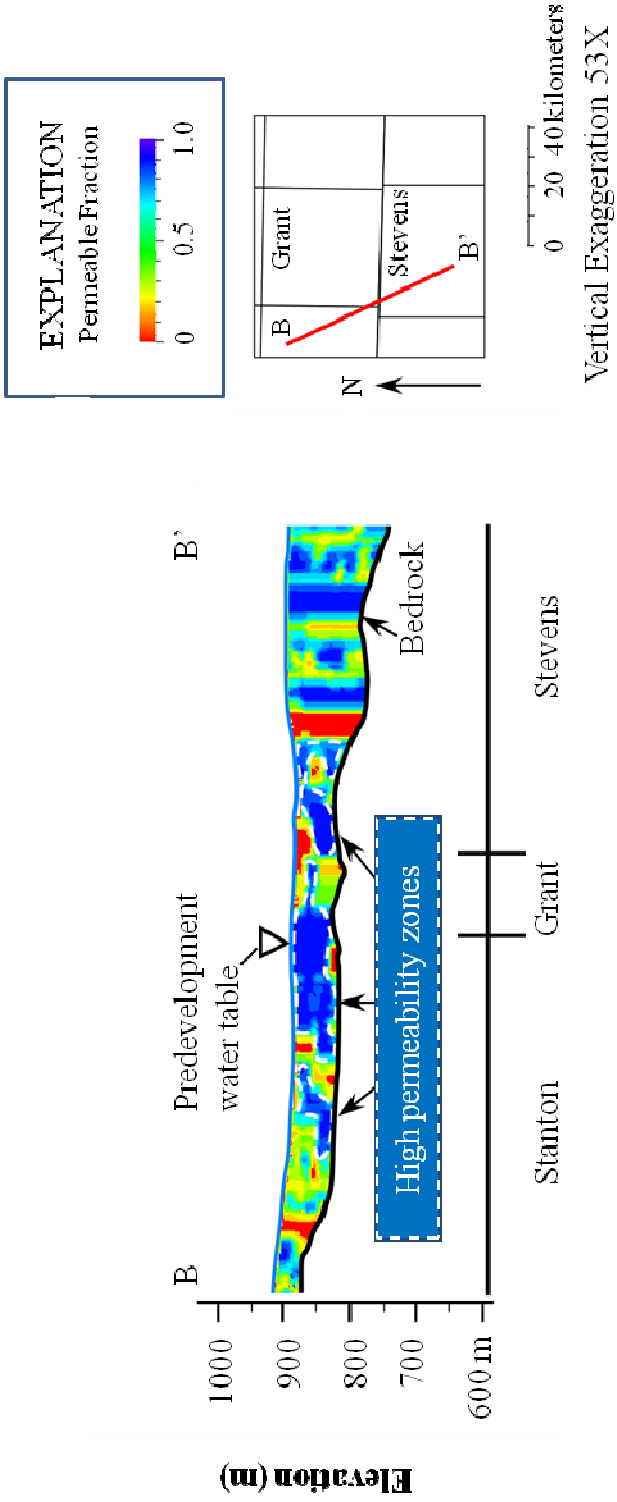

Figure 5.48. Profile diagram illustrates the distribution of permeable fraction along line B-B'.

a

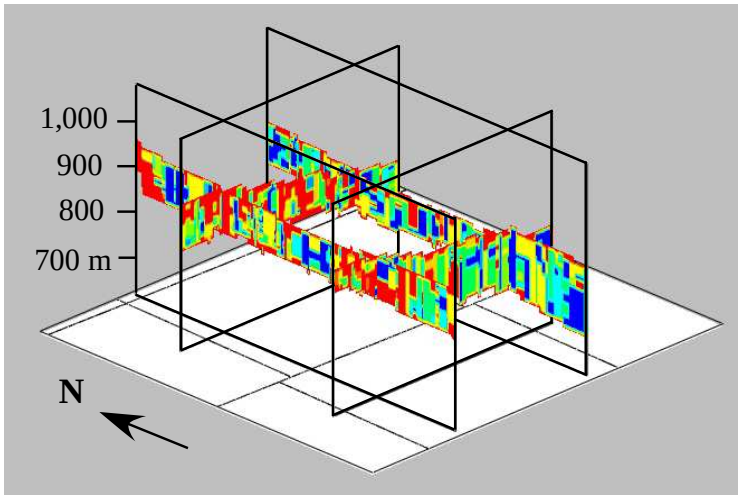

b

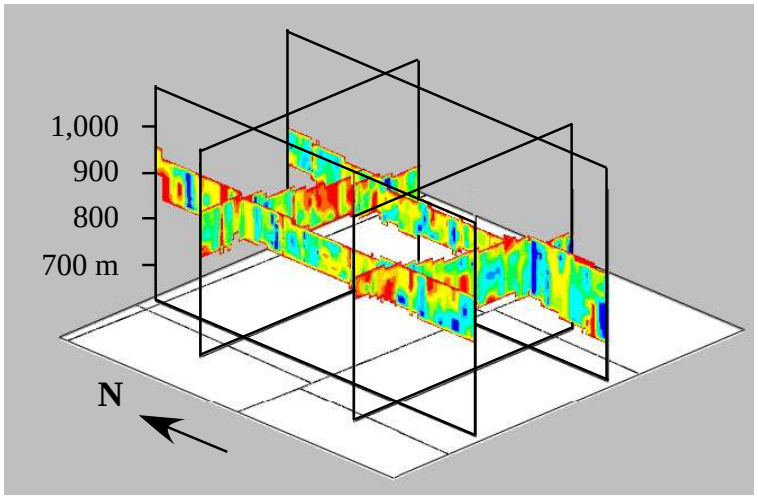

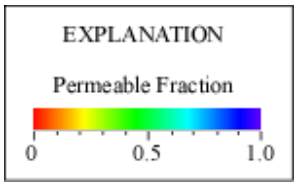

Figure 5.49. Comparison of (a) unsmoothed and (b) smoothed permeable fraction distributions generated using the closest point algorithm.

Based on permeable fraction, estimates of hydraulic conductivity are used as input for the ground-water flow model. Values of hydraulic conductivity initially assigned to the TPROGS indicator variables differ by an order of magnitude to emphasize gross differences in hydrogeologic properties. Very fine, fine, medium, and coarse unconsolidated sediments are assigned initial hydraulic conductivity values of 0.1, 1, 10, and 100 m/d, respectively. The hydraulic conductivity estimates fall within the range of values published by Gutentag et al. (1984) for similar deposits. Appendix B summarizes the hydraulic conductivity values assigned to different sediment types represented in the study. In Figure 5.410, cross plots of permeable fraction values and log-transformed regional hydraulic conductivity estimates from (a) Liu et al. (2010) and (b) Gutentag et al. (1984) show the relationship between sediment types and hydrogeologic properties in the study area.

(a)

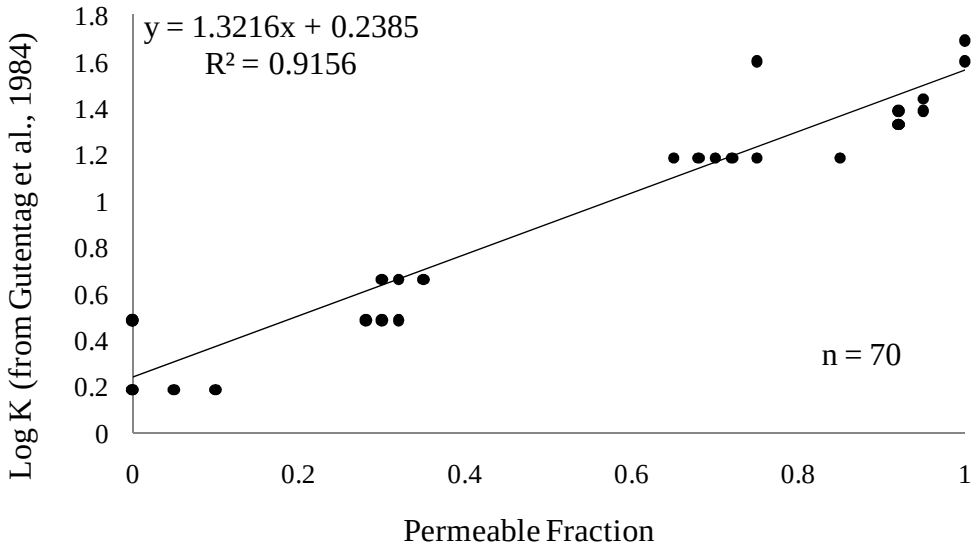

(b)

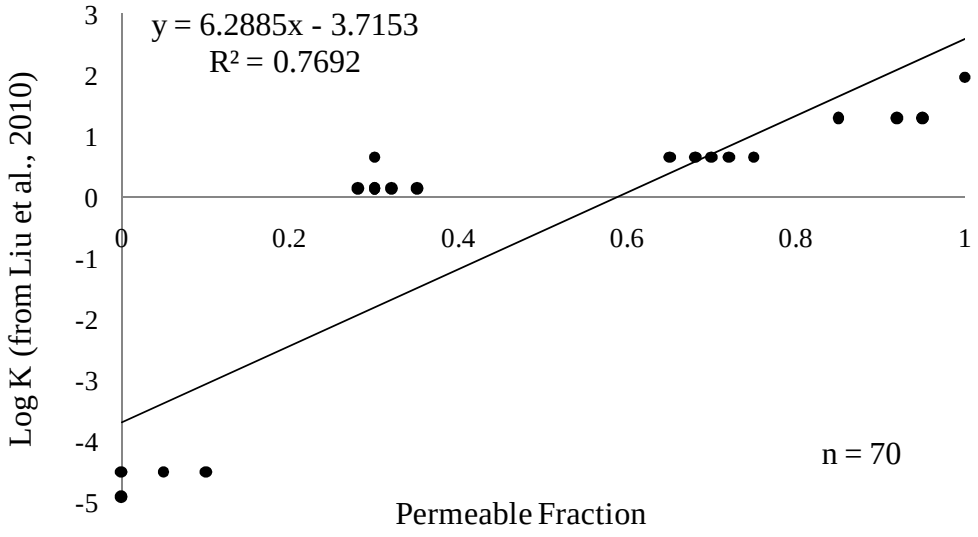

Figure 5.410. Cross plot of permeable fraction and logK values derived from studies by (a) Liu et al. (2010) and (b) Gutentag et al. (1984).

5.5 Modeling

As discussed in Section 4.5, the steady-state calibration procedure in MODFLOW involves the adjustment of boundary conditions, conductance, and hydraulic conductivity values to minimize the model error. Uncertainty in the model input parameters is attributed to the limited accuracy of predevelopment measurements and, more importantly, to the spatial heterogeneity in aquifer characteristics. Results of the steady-state simulations demonstrate the influence of spatial variability on the groundwater flow system. The calibrated model simulates ground-water flow in the observed directions, generally from the west to the east and southeast. Appendix F presents the hydraulic head residuals resulting from the calibration of 16 different ground-water model scenarios.

Figure 5.51 compares the measured potentiometric surface with simulated hydraulic head contours for predevelopment conditions in the homogeneous simulation M5. The results of the heterogeneous, two layer flow simulation illustrate the increasing complexity of the flow field. The potentiometric surface and direction of flow is affected by changes in the spatial distribution of hydrogeologic properties across the region. Figure 5.52 compares the measured predevelopment potentiometric surface with simulated contours from the heterogeneous simulation T8. In both the homogeneous and heterogeneous scenarios, the simulated predevelopment water-levels are similar to the input potentiometric contours.

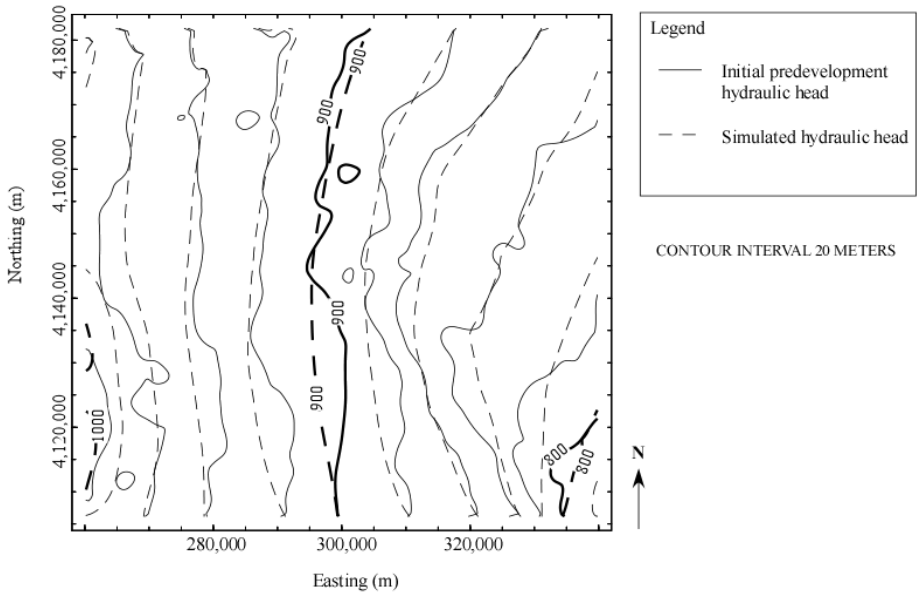

Figure 5.51. Results from the steady-state, homogeneous ground-water flow simulation M5.

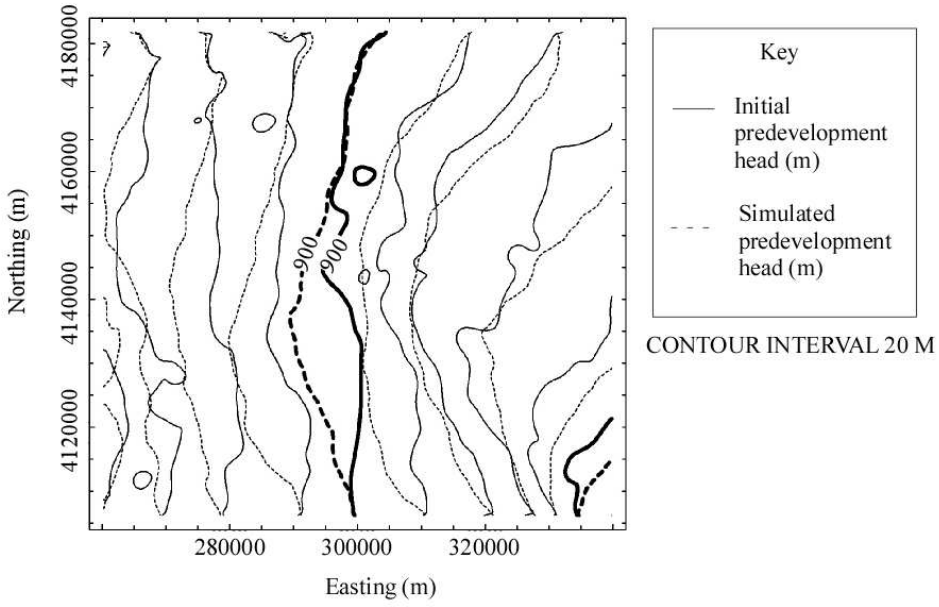

Figure 5.52. Initial and simulated predevelopment hydraulic heads for the heterogeneous, steady-state simulation T8.

6.0 Interpretations and Discussion

The capacity of the aquifer system to transmit water is influenced, in part, by the spatial distribution and continuity of permeable and non-permeable deposits that form hydrostratigraphic units. In southwest Kansas, the complex distribution of lithology is attributed to a variety of geologic processes that influenced the region during the Neogene. Although variable in quality, drilling logs prepared in the field are typically the most abundant source of subsurface information for hydrogeologic investigations in the Neogene sequence of southwest Kansas (Macfarlane, 2009). The quality of information in a drilling log generally depends on the ability of the driller to accurately describe the drill cuttings and determine the depths of the bedrock surface and changes in lithology. Appropriate use of the conceptual information contained in drilling logs lies in recognizing limitations of the data and applying flexible approaches to consistently translate material descriptions into a form useful for 2D and 3D visualization. Overall, the descriptions from the test-hole logs compare favorably with corresponding KGS sample logs. Spot checks of drilling logs show consistency between lithologic observations recorded by different drillers.

As expected with most interpolation algorithms, kriging produces a smooth and relatively featureless parameter field. Uncertainty is often underestimated because the kriging estimates do not take into account the inherent uncertainty associated with fitting the semivariogram model to the empirical data. Although kriging methods are useful for representing regional trends, simulation techniques are generally better for rendering local features because they account for the covariance between the different estimates, as well as the reduced variability in the model. Stochastic simulation methods are more versatile than traditional interpolation algorithms in reproducing spatial patterns in the data and accounting for different types and sources of data

(Deutsch and Journel, 1992). The transition probability-based geostatistical approach maximizes theoretical potential by conceptualizing geostatistical models in a more interpretive framework than a semivariogram approach. Markov chain models provide a straight-forward and mathematically-simple stochastic model that accounts for all spatial cross-correlations between categorical data.

A simple, steady-state flow simulation incorporated different lithology-based distributions of hydrogeologic properties to evaluate the sensitivity of the ground-water flow system to variations in the hydraulic conductivity field. Sources of uncertainty in the calibrated simulation include an incomplete knowledge of the spatial distribution of lithology and hydraulic conductivity, boundary conditions, input parameters, and conceptual model uncertainty (Anderson and Woessner, 1992). The MODFLOW results show that the flow system is sensitive to variations in the spatial distribution and connectivity of permeable units. The small differences between correlation values in Appendix F suggest that detailed approximations of parameter distributions are not necessary to represent the hydrostratigraphic framework.

Calibration of the flow simulation could possibly be improved with higher-resolution data, such as increasing the spatial discretization of hydraulic conductivity. However, without additional field data, finer discretization is not possible. In addition, combinations of parameter values other than those used in the study also may give satisfactory results. One approach to improving the analysis is to use the distribution of residuals to inform geostatistics. Residual distribution maps show areas of overestimation and underestimation. The residuals can be implemented in an automated, iterative process to minimize the objective function and refine estimates of hydrogeologic property distributions.

7.0 Conclusions

The thickness, distribution, and hydrogeologic properties of lithologic units are highly variable across the study area, and significantly affect local ground-water flow and availability. Complexity in the spatial distribution of lithology is attributed to alternating periods of erosion, deposition, and stability during the Neogene and Quaternary, as well as subsequent depositional, erosional, and pedogenic processes in a semiarid environment. Although drill cuttings and outcrop studies are insufficient for direct lateral correlation across the study area, it is possible to generate spatial approximations of subsurface heterogeneity based on interpretations from irregularly-spaced well log data using various data-based approaches that differ in operation, the type of information needed, and computational requirements.

Using a relational database of over 4,000 drilling logs, the study focused on finding the most effective methods for translating conceptual information from drilling logs into a form useful for hydrostratigraphic characterization. Queries enable data filtering and retrieval, and demonstrate the functionality of the database. Semivariogram and transition probability models fit to the empirical indicator and mean permeable fraction data show that low permeability deposits like clay and silt can be spatially correlated at distances of up to 1 km across the study area. Similarly, high permeability sediments can be traced at distances up to 800 m. The correlation length of sand and gravel deposits establishes a sense of scale to the channel width, while the greater correlation length of fine-grained mud and silt may correspond to more laterally extensive floodplain deposits.

The ground-water flow model described in this report incorporates various spatial approximations of hydraulic conductivity to assess the influence of spatial variability on the ground-water flow system. Results of the ground-water flow simulation should be interpreted

with caution, as the ground-water flow model is only an approximation of the aquifer system. Furthermore, the solution obtained from model calibration is not necessarily unique in that any number of reasonable variations in model parameters may produce equally acceptable results. Sources of uncertainty in the model include an incomplete knowledge of aquifer parameters and simplifying assumptions used in the formulation and simulation of ground-water flow equations. Significant conclusions resulting from this study are (1) carefully-screened drilling logs provide an abundant source of supplementary information for hydrogeologic studies in southwestern Kansas, (2) hydrogeologic units are discontinuous and highly variable across the study area, (3) indicator approaches and transition probability-based geostatistics are useful for rendering detailed approximations of spatial variability, and (4) fine-grained deposits are the most laterally extensive and most commonly described sediment types in the study area.

References

Anderson, M.P., and Woessner, W.W., 1992, Applied groundwater modeling: Simulation of flow and transport: Academic Press, New York, 381 p.

Bass, N.W., 1926, Geologic investigations in western Kansas: Kansas Geological Survey Bulletin 11, p. 53-89.

Bohling, G.C., 2005, Introduction to geostatistics and variogram analysis [Class handout]: CPE 940, University of Kansas, Lawrence, Kansas, 20 p.

Bohling, G.C., 2005b, Kriging [Class handout]: CPE 940, University of Kansas, Lawrence, KS, 20 p.

Bohling, G. C., and Wilson, B. B., 2005, Statistical and geostatistical analyses of the Kansas High Plains water table elevations, 2005 measurement campaign: Kansas Geological Survey Open File Report 2005-6, 43 p.

Carle, S. F., 1996, A transition probability-based approach to geostatistical characterization of hydrostratigraphic architecture: Ph. D. dissertation, University of California, Davis, 248 p.

Carle, S.F., and Fogg, G.E., 1996, Transition probability-based indicator geostatistics: Mathematical Geology, v. 28, no. 4, p. 453–476.

Carle, S. F., and Fogg, G.E., 1997, Modeling spatial variability with one and multidimensional continuous-lag Markov chains: Mathematical Geology, v. 29, no. 7, p. 891-918.

Carle, S.F., 1998, Transition probability geostatistical software, version 2.0: User's manual: University of California, Davis.

Carle, S.F., Labolle, E.M., Weissmann, G.S., Van Brocklin, D., and Fogg, G.E., 1998, Conditional simulation of hydrofacies architecture: A transition probability/Markov approach, *in*, Fraser, G.S., and Davis, J.M., eds., Hydrogeologic Models of Sedimentary Aquifers, Concepts in Hydrogeology and Environmental Geology No. 1: SEPM Special Publication, p. 147–170.

Carle, S.F., 1999, T-PROGS: transition probability geostatistical software version 2.1: Hydrologic Sciences Graduate Group University of California, Davis.

Darton, N.H., 1920, Description of the Syracuse and Lakin quadrangles: U.S. Geological Survey Bulletin 691, p. 1-26.

de Marsily, G., Delay, F., Goncalvès, J., Renard, P., Teles, V., and Violette, S., 2005, Dealing with spatial heterogeneity: Hydrogeology Journal 13, no. 1: p. 161-183.

Deutsch, C.V., and Journel, A. J., 1992, Geostatistical software library and user's guide: Oxford University Press, New York, 340 p.

Doherty, J., 2004, PEST Model-Independent Parameter Estimation: Watermark Numerical Computing, Australia.

Domenico, P.A., and Schwartz, F.W., 1990, Physical and chemical hydrogeology: John Wiley and Sons, New York, 824 p.

Dugan, J. T., and Peckenpaugh, J. M., 1985, Effects of climate, vegetation, and soils on consumptive water use and ground-water recharge to the Central Midwest regional aquifer system, midcontinent United States: U.S. Geological Survey, Water Resources Investigations Report 85-4236, 78 p.

Fader, S.W., Gutentag, E.D., Lobmeyer, D.H., and Meyer, W.R., 1964, Geohydrology of Grant and Stanton counties, Kansas: Kansas Geological Survey Bulletin 168, 147 p.

Fenneman, N.M., 1946, Physical subdivisions of the United States (Map): U.S. Geological Survey, 1:700,000, 1 sheet.

Frye, J.C., 1942, Geology and ground-water resources of Meade County, Kansas: Kansas Geological Survey, Bulletin 45, 152 p.

Frye, J.C., 1946, The High Plains surface in Kansas: Kansas Academy of Science, Transactions, v. 49, no. 1, p. 71-86.

Frye, J.C., 1950, Origin of Kansas Great Plains Depressions: Kansas Geological Survey, Bulletin 86.

Frye, J.C., and Leonard, A.B., 1952, Pleistocene geology of Kansas: Kansas Geological Survey Bulletin 99, 230 p.

Frye, J.C., Leonard, A.B., and Swineford, A., 1956, Stratigraphy of the Ogallala Formation (Neogene) of northern Kansas: Kansas Geological Survey, Bulletin 118, 92 p.

Gustavson, T.C., 1996, Fluvial and eolian depositional systems, paloesols, and paleoclimate of the upper Cenozoic Ogallala and Blackwater Draw formations, southern High Plains, Texas and New Mexico: Bureau of Economic Geology Report of Investigations 239, 62 p.

Gutentag, E.D., 1963, Studies of the Pleistocene and Pliocene deposits in southwestern Kansas: Kansas Academy of Science, Transactions, v. 66, n. 4, p. 606-621.

Gutentag, E.D., Lobmeyer, D.H., and Slagle, S.E., 1981, Geohydrology of southwestern Kansas: Kansas Geological Survey, Irrigation Series 7, 73 p.

Gutentag, E.D., Heimes, F.J., Krothe, N.C., Luckey, R.R., and Weeks, J.B., 1984, Geohydrology of the High Plains aquifer in parts of Colorado, Kansas, Nebraska, New Mexico, Oklahoma, South Dakota, Texas, and Wyoming: U.S. Geological Survey Professional Paper 1400-B, 63 p.

Hibbard, C.W., 1953, The insectivores of the Rexroad fauna, upper Pliocene of Kansas: Journal of Paleontology, v. 27, no.1, p. 21-32.

Hibbard, C.W., 1958, New stratigraphic names for early Pleistocene deposits in southwestern Kansas: American Journal of Science, v. 256, no. 1, p. 54-59.

Isaaks, E.H. and Srivastava, R.M., 1989. An introduction to applied geostatistics: New York, Oxford University Press, 561 p.

Jones, N.L., Walker, J.R., and Carle, S.F. 2002, Using transition probability geostatistics with MODFLOW: ModelCARE 2002: Proceeding of the Fourth International Conference on Calibration and Reliability in Groundwater Modelling, Prague, Czech Republic, 17-20 June 2002, vol. I, p. 295-298.

Kansas Department of Agriculture (KSDA), 2004, Rules and regulations: Southwest Kansas Groundwater Management District No. 3: Kansas Department of Agriculture, Division of Water Resources, 13 p., http://www.ksda.gov/includes/statute_regulations/mainportal/GMD3.pdf.

Kansas Water Resources Board (KWRB), 1958, Preliminary appraisal of Kansas water problems, see.2 Cimarron Unit: Kansas Water Resources Board, State Water Plan Studies, pt. A, p. 1-124.

Kitanidis, P.K., 1997, Introduction to geostatistics: Applications in hydrogeology, 249 p.

Koltermann, C. E. and Gorelick, S. M., 1996, Heterogeneity in sedimentary deposits: A review of structure-imitating, process imitating, and descriptive approaches: Water Resources Research, v. 32, p. 2617–2658.

Kume, J., and Spinazola, J.M., 1985, Geohydrology of sandstone aquifers in southwestern Kansas: Kansas Geological Survey, Irrigation Series 8, 49 p.

Latta, B.F., 1941, Geology and ground-water resources of Stanton County, Kansas: Kansas Geological Survey, Bulletin 37, 119 p.

Leonard, E.M., 2002, Geomorphic and tectonic forcing of late Neogene warping of the Colorado piedmont: Geology, vol. 30, no. 7, p. 595-598.

Liu, G., Whittemore, D.O., Wilson, B.B., Butler, J.J., Jr., 2010, Modeling the High Plains aquifer in southwest Kansas: From the Past to the Future, Proceedings 27th Annual Water and Future of Water Conference, Topeka, KS, 26 October 2010.

Lin, C., and Harbaugh, J. W., 1984, Graphic display of two- and three- dimensional Markov computer models in geology: Van Nostrand Reinhold, New York, 180 p.

Long, A.J., Putnam, L.D., and Carter, J.M., 2003, Simulated ground-water flow in the Ogallala and Arikaree aquifers, Rosebud Indian Reservation Area, South Dakota, U.S. Geological Survey Water-Resources Investigations Report 03-4043, 69 p.

Luckey, R. L., Gutentag, E. D., Heimes, F. J., and Weeks, J. B., 1986, Digital simulation of ground-water flow in the High Plains aquifer in parts of Colorado, Kansas, Nebraska, New Mexico, Oklahoma, South Dakota, Texas, and Wyoming: U.S. Geological Survey, Professional Paper 1400-D, 57 p.

Luckey, R. L., and Becker, M. F., 1999, Hydrogeology, water use, and simulation of flow in the High Plains aquifer in northwestern Oklahoma, southeastern Colorado, southwestern Kansas, northeastern New Mexico, and northwestern Texas: U.S. Geological Survey, Water-Resources Investigations Report 99-4104, 68 p.

Ludvigson, G.A., Sawin, R.S., Franseen, E.K., Watney, W.L., West, R.R. and Smith, J.J., 2009, A review of the stratigraphy of the Ogallala Formation and revision of Neogene ("Tertiary") nomenclature in Kansas: *in*, Current Research in Earth Sciences: Kansas Geological Survey, Bulletin 256, part 2, http://www.kgs.ku.edu/Current/2009/Ludvigson/index.html.

Macfarlane, P. A., Whittemore, D. O., Townsend, M. A., Doveton, J. H., Hamilton, V. J., Coyle, W. G., III, and Wade, A., 1990, The Dakota Aquifer Program annual report, FY89: Kansas Geological Survey, Open-file Report 90-27, 302 p.

Macfarlane, P.A., 1993, The effect of topographic relief and hydrostratigraphy on the upper part of the regional groundwater flow system in southeastern Colorado and western and central Kansas, with emphasis on the Dakota aquifer: Ph.D. dissertation, University of Kansas, Lawrence, 197 p.

Macfarlane, P.A., 2000, Revisions to the nomenclature for Kansas aquifers: Kansas Geological Survey, Bulletin 244, pt.2, 14 p.

Macfarlane, P.A., Wilson, B.B., and Bohling, G., 2005, Practical saturated thickness of the Ogallala aquifer in two small areas of Southwest Kansas Groundwater Management District 3: Kansas Geological Survey, Open-file Report 2005-29, 33p.

Macfarlane, P.A., and Wilson, B.B., 2006, Enhancement of the bedrock surface-elevation map beneath the Ogallala portion of the High Plains aquifer, western Kansas: Kansas Geological Survey, Technical Series 20, 28 p. and 2 map plates.

Macfarlane, P.A., and Schneider, N., 2007, Distribution of the permeable fraction and practical saturated thickness in the Ogallala portion of the High Plains aquifer in the southwest

Kansas Groundwater Management District 3: Kansas Geological Survey Open-file Report 2007-28, 70 p.

Macfarlane, P.A., 2009, New insights into the hydrostratigraphy of the High Plains aquifer from three-dimensional visualizations based on well records: Geosphere, v. 5, no. 1, p. 51-58.

McGuire, V.L., 2009, Water-level changes in the High Plains aquifer, predevelopment to 2007, 2005-06, and 2006-07: U.S. Geological Survey Scientific Investigations Report 2009-5019.

McLaughlin, T.G., 1946, Geology and ground-water resources of Grant, Haskell, and Stevens Counties, Kansas: Kansas Geological Survey Bulletin 61, p. 1-221, pls. 1-12, figs. 1-18.

McMillan, M.E., Angevine, C.L., and Heller, P.L., 2002, Postdepositional tilt of the Miocene-Pliocene Ogallala Group on the western Great Plains: evidence of late Cenozoic uplift of the Rocky Mountains: Geology, v. 30, p. 63-66.

McMillan, M.E., Heller, P.L., and Wing, S.L., 2006, History and causes of post-Laramide relief in the Rocky Mountain orogenic plateau: Geological Society of America Bulletin, v. 118, p. 393–405.

Merriam, D. F., and Frye, J. C., 1954, Additional studies of the Cenozoic of western Kansas: Kansas Geological Survey, Bulletin 109, pt. 4, p. 49-64.

Molnar, P., 2004, Late Cenozoic increase in the accumulation rates of terrestrial sediment: How might climate change have affected erosion rates? Annual Reviews Earth Planet Science, v. 32, p. 67-89.

Moore, R. C., Frye, J.C., Jewett, J.M., Lee, Wallace, and O'Connor, H.G., 1951, The Kansas rock column: Kansas Geological Survey, Bulletin 89, 132 p., http://www.kgs.ku.edu/Publications/Bulletins/89/index.html.

Olea, R.A., and Davis, J.C., 2003, Geostatistical analysis and mapping of water-table elevations in the High Plains aquifer of Kansas after the 2003 monitoring season: Kansas Geological Survey Open-file Report 13.

Pazzaglia, F.J., and Hawley, J.W., 2004, Neogene (rift flank) and Quaternary geology and geomorphology, *in*, Mack, G., and Giles, K., eds., The Geology of New Mexico: New Mexico Geological Society Special Publication 11, Albuquerque, NM, p. 407-437.

Pebesma, E.J., and Wesseling, C.G., 1998, Gstat: a program for geostatistical modeling, prediction and simulation: Computers and Geosciences, v. 24, no. 1, p. 17-31.

Politis, D. N., 1994, Markov chains in many dimensions: Advances in Applied Probability, v. 26, no. 3, p. 756-774.

RockWare, 2009, RockWorks v.14: Golden, CO.

Ross, C. G., 1989, LEO-conversion between legal and geographic reference systems in Kansas: Kansas Geological Survey, Open-file Report 89-10, 9 p.

Seni, S.J., 1980, Sand-body geometry and depositional systems, Ogallala formation, Texas: Texas Bureau of Economic Geology Report of Investigations 105, 36 p.

Smith, H.T.U., 1940, Geologic studies in southwestern Kansas: Kansas Geological Survey Bulletin 34, 212 p.

Sophocleous, M.A., 2005. Groundwater recharge and sustainability in the High Plains aquifer in Kansas, USA: Hydrogeology Journal, 13(2): 351-365.

Stullken, L.E., Watts, K.R., and Lindgren, R.J., 1985, Geohydrology of the High Plains aquifer, western Kansas: U.S. Geological Survey, Open-file Report 85-4198, 86 p.

Trimble, D.E., 1980, Neogene tectonic history of the Great Plains contrasted with that of the southern Rocky Mountains – a synthesis: The Mountain Geologist, v. 17, no. 3, p. 59-69.

Watts, K.R., 1985, Potential hydrologic effects of ground-water withdrawals from the Dakota aquifer, southwestern Kansas: U.S. Geological Survey Water-Supply Paper 2304, 47 p.

Weissmann, G.S., Carle, S.F., and Fogg, G.E., 1999, Three-dimensional hydrofacies modeling based on soil surveys and transition probability geostatistics: Water Resources Research 35:1761–1770.

Weissmann, G.S., and G.E. Fogg, 1999, Multi-scale alluvial fan heterogeneity modeled with transition probability geostatistics in a sequence stratigraphy framework: Journal of Hydrology. 226(1–2):48–65.

Weissmann, G.S., Zhang, Y., LaBolle, E.M., and Fogg, G.E., 2002, Dispersion of groundwater age in an alluvial aquifer system: Water Resources Research 38(10), 1198.

Whittemore, D. O., Grieve, E. R., Young, D. P., Wilson, B. B., 2005, Water Quality in the High Plains Aquifer and the Cimarron River in Seward and Meade Counties, Kansas: Kansas Geological Survey Open-file Report 27, 36 p.

Wilson, B.B., 2007, Ground-Water Levels in Kansas: Kansas Geological Survey, Open-file Report 2007-1.

Wilson, B.B., Young, D.P., and Buddemeier, R.W., 2002, Exploring relationships between water table elevations, reported water use, and aquifer lifetime as parameters for consideration in aquifer subunit delineations: Kansas Geological Survey, Open-file Report 2002-25D.

Young, D.P., Bartley, J.D., Wilson, B.B., Misgna, G., 2003, Dynamic online access to the High Plains aquifer section-level database: Kansas Geological Survey, Open-file Report 2003-38.

Young, D.P., Macfarlane, P.A., Whittemore, D.O., and Wilson, B.B., 2005, Hydrogeologic characteristics and hydrologic changes in the Cimarron River basin, southwestern Kansas: Kansas Geological Survey, Open-file Report 2005-26, 41 p.

Appendix A: Regional Estimates of Hydrogeologic Properties

The proceeding tables contain estimates of hydrogeologic properties published in previous studies.

Table A-1. Hydraulic parameters from previous studies

County	Northing (m)	Easting (m)	K (m\d)	S or Sy	ST (m)	T (m^2\d)	Geologic source	Reference
Kearny	4182500	291682	11	6.0×10^{-4}	55	585	QT	Gutentag et al. (1972)
Haskell	4173777	320471	56	0.18	43	2,415		Gutentag and Stullken (1974)
Grant	4174263	302730	27	1.4×10^{-4}	71	1,905	Npl, No	Fader et al. (1964)
Grant	4171398	288496	10	1.2×10^{-4}	67	650	Npl, No	Fader et al. (1964)
Grant	4175170	283427	12	2.3×10^{-4}	64	790	Npl, No	Fader et al. (1964)
Grant	4173302	278164	89	4.8×10^{-3}	82	7,330	Npl, No	Fader et al. (1964)
Grant	4173577	282993	29	3.5×10^{-4}	68	1,979	Npl, No	Fader et al. (1964)
Grant	4173503	285019	15	2.1×10^{-4}	59	883	Npl, No	Fader et al. (1964)
Grant	4171269	278911	30	2.4×10^{-3}	79	2,332	Npl, No	Fader et al. (1964)
Stanton	4172474	266175	22	4.8×10^{-3}	76	1,700	Npl, No	Fader et al. (1964)
Grant	4167378	303355	41	2.2×10^{-4}	66	2,676	Npl, No	Fader et al. (1964)
Grant	4167050	285277	7	2.8×10^{-4}	91	632	Npl, No	Fader et al. (1964)
Grant	4165520	282055	15	6.0×10^{-3}	98	1,477	Npl, No	Fader et al. (1964)
Grant	4163099	282389	17	2.1×10^{-4}	89	1,551	Npl, No	Fader et al. (1964)
Stanton	4167722	276458	12	1.1×10^{-4}	43	502	Npl	Fader et al. (1964)
Stanton	4164699	269545	36	9.5×10^{-4}	65	2,332	Npl, No	Fader et al. (1964)
Stanton	4163624	275541	66	9.5×10^{-3}	87	5,779	Npl, No	Fader et al. (1964)
Grant	4155924	311527	23	3.8×10^{-4}	73	1,663	Npl	Fader et al. (1964)
Grant	4150985	284097	6	9.4×10^{-4}	98	557	Npl, No	Fader et al. (1964)
Stanton	4154026	276515	10	1.1×10^{-3}	75	725	Npl, No	Fader et al. (1964)
Grant	4149907	293318	4	1.4×10^{-4}	99	372	Npl, No	Fader et al. (1964)
Grant	4145271	287592	9	2.9×10^{-4}	74	697	Npl	Fader et al. (1964)
Grant	4142680	293960	20	3.2×10^{-3}	88	1,802	Npl, No	Fader et al. (1964)
Grant	4143546	277464	45	4.4×10^{-4}	94	4,190	Npl, No	Fader et al. (1964)

Npl, Pleistocene; No, Ogallala; QT, Quaternary

Italicized wells do not extend to bedrock.

Appendix B: Lithology Types and Associated Hydrogeologic Parameters

The proceeding table contains the terms assigned to lithology types identified in the relational lithology database, along with their associated regional hydrogeologic properties.

Table B-1. Lithology terms and corresponding hydraulic property estimates.

#	Terms	Lithology	K^1 (m\d)	K^2 (m\d)	S_y	Relative Permeability	n	Proportion (%)
1	sh	shale	1.22×10^{-5}	1.52	0.05	0	3012	3.47
2	c	clay	1.22×10^{-5}	1.52	0.05	0	2453	28.3
3	coal	coal	1.22×10^{-5}	3.05	0.05	0	0	0
4	br	bedrock	1.22×10^{-5}	3.05	0.05	0	0	0
5	rb	red bed	1.22×10^{-5}	3.05	0.05	0	416	0.48
6	r	rock	1.22×10^{-5}	3.05	0.05	0	2038	2.35
7	sst	siltstone	1.22×10^{-5}	1.52	0.05	0	4	0
8	fsc	fine silty clay	3.05×10^{-5}	1.52	0.08	0	30	0.03
9	fmsc	fine to medium silty clay	3.05×10^{-5}	1.52	0.08	0	1	0
10	sc	silty clay	3.05×10^{-5}	1.52	0.08	0	208	0.24
11	msc	medium silty clay	3.05×10^{-5}	1.52	0.08	0	2	0
12	fcrssc	fine to coarse silty clay	3.05×10^{-5}	1.52	0.08	0	2	0
13	mcrssc	medium to coarse silty clay	3.05×10^{-5}	1.52	0.08	0	1	0
14	fsdc	fine sandy clay	3.05×10^{-5}	4.57	0.08	0.3	1	0
15	fmsdc	fine to medium sandy clay	3.05×10^{-5}	4.57	0.08	0.3	1	0
16	msdc	medium sandy clay	3.05×10^{-5}	4.57	0.08	0.3	0	0
17	sdc	sandy clay	3.05×10^{-5}	4.57	0.08	0.3	9889	11.40
18	fcrssdc	fine to coarse sandy clay	3.05×10^{-5}	4.57	0.08	0.3	0	0.00
19	mcrssdc	medium to coarse sandy clay	3.05×10^{-5}	4.57	0.08	0.3	0	0.00
20	cs	clayey silt	3.05×10^{-5}	1.52	0.08	0	0	0.00
21	fs	fine silt	3.05×10^{-5}	1.52	0.08	0	0	0.00
22	s	silt	3.05×10^{-5}	1.52	0.08	0	524	0.60
23	ts	top soil	3.05×10^{-5}	1.52	0.08	0	2934	3.38
24	o	overburden	3.05×10^{-5}	1.52	0.08	0	74	0.09

Table B-1. Lithology terms and corresponding hydraulic property values

#	Synonymy	Lithology	K^1 (m\d)	K^2 (m\d)	S_y	Permeable Fraction	n	Proportion (%)
25	m	marl	3.05×10^{-5}	3.05	0.08	0	291	0.34
26	ca	calcified material	3.05×10^{-5}	3.05	0.08	0	4427	5.10
27	fds	fine sandy silt	1.34	3.05	0.08	0.3	3	0
28	fmds	fine to medium sandy silt	1.34	3.05	0.08	0.3	0	0
29	mds	medium sandy silt	1.34	3.05	0.08	0.3	0	0
30	sds	sandy silt	1.34112	3.05	0.08	0.3	0	0
31	fcrsds	fine to coarse sandy silt	1.34112	3.05	0.08	0.3	0	0
32	mcrsds	medium to coarse sandy silt	1.34112	3.05	0.08	0.3	0	0
33	crsds	coarse sandy silt	1.34112	3.05	0.08	0.3	0	0
34	gc	gravelly clay	1.34112	4.57	0.08	0.3	5	0.01
35	ss	sandstone	1.34112	3.05	0.08	0	3158	3.64
36	csnd	clayey sand	4.4196	15.24	0.16	0.7	0	0.00
37	fss	fine silty sand	4.4196	15.24	0.16	0.7	11	0.01
38	fmss	fine to medium silty sand	4.4196	15.24	0.16	0.7	7	0.01
39	ssnd	silty sand	4.4196	15.24	0.16	0.7	35	0.04
40	mss	medium silty sand	4.4196	15.24	0.16	0.7	0	0
41	fcrsss	fine to coarse silty sand	4.4196	15.24	0.16	0.7	1	0
42	mcrsss	medium to coarse sandy silt	4.4196	3.05	0.16	0.3	0	0
43	crsss	coarse silty sand	4.4196	15.24	0.16	0.7	1	0
44	u	unknown	4.4196	3.05	0.16	0	60	0.07
45	cesd\cg	cemented sand and\or gravel	4.4196	3.05	0.16	0	953	1.10
46	fsnd	fine sand	4.572	15.24	0.24	1	5481	6.32
47	fmsnd	fine to medium sand	4.572	21.34	0.24	1	3584	4.13
48	snd	sand	19.2024	24.38	0.24	1	6937	7.99

Table B-1. Lithology terms and corresponding hydraulic property values

#	Synonymy	Lithology	K [1]	K [2]	S_y	Permeable	n	Proportion
49	msnd	medium sand	19.2024	24.38	0.24	1	1405	1.62
50	fcrssnd	fine to coarse sand	19.2024	21.34	0.24	1	3127	3.60
51	fmcrssnd	fine to medium coarse sand	19.2024	21.34	0.29	1	69	0.08
52	mcrssnd	medium to coarse sand	19.2024	27.43	0.24	1	2005	2.31
53	crssnd	coarse sand	19.2024	27.43	0.29	1	1827	2.11
54	cg	clayey gravel	19.2024	39.62	0.24	0.7	0	0
55	sg	silty gravel	19.2024	39.62	0.29	0.7	45	0.05
56	fsdg	fine sand and gravel	91.1352	39.62	0.29	1	9	0.01
57	fmsdg	fine to medium sand and	91.1352	48.77	0.29	1	1912	2.20
58	msdg	medium sand and gravel	91.1352	48.77	0.29	1	181	0.21
59	sdg	sand and gravel	91.1352	48.77	0.29	1	1250	1.44
60	fcrssdg	fine to coarse sand and gravel	91.1352	48.77	0.29	1	62	0.07
61	mcrssdg	medium to coarse sand and	91.1352	48.77	0.29	1	152	0.18
62	crssdg	coarse sand and gravel	91.1352	48.77	0.29	1	73	0.08
63	fcrssg	fine to coarse sandy gravel	91.1352	48.77	0.29	1	0	0
64	fg	fine gravel	91.1352	76.20	0.29	1	2166	2.50
65	fmg	fine to medium gravel	91.1352	76.20	0.29	1	682	0.79
66	mg	medium gravel	91.1352	91.44	0.29	1	366	0.42
67	g	gravel	91.1352	91.44	0.29	1	1913	2.20
68	fcrsg	fine to coarse gravel	91.1352	91.44	0.29	1	340	0.39
69	mcrsg	medium to coarse gravel	91.1352	106.7	0.29	1	248	0.29
70	crsg	coarse gravel	91.1352	106.7	0.29	1	322	0.37

K [1] Liu et al., 2010
K [2] Gutentag et al., 1984

Appendix C: Parameter Input Files

The following parameter input files contain all the settings used to generate spatial approximations and simulations of hydrogeologic parameters.

```
GAMEAS
# The GAMEAS program in TPROGS calculates vertical and horizontal transition probabilities.

START OF PARAMETERS
PST3mSubSlim.dat                    /input file
1 2 3                               /x, y, z columns
4 4 5 6 7                           /nvar, var 1,2,3,…columns
-1. 2.                              /vmin, vmax
PST3mSubTpv.dat                     /output file
55                                  /nlags
10                                  /lag spacing
5                                   /lag tolerance
1                                   /ndir
0.0   90.  0.01   -90   0.01   0.0  /az, daz, azbw, dip, aztol, dtol
16                                  /number of bivariate statistics
1 1  11                             /j, k, 11=tp
1 2  11
1 3  11
1 4  11
2 1  11
2 2  11
2 3  11
2 4  11
3 1  11
3 2  11
3 3  11
3 4  11
4 1  11
4 2  11
4 3  11
4 4  11
```

MCMOD

The MCMOD program in TPROGS is a 3D Markov chain modeling program. The parameter file contains the input for an embedded Markov chain analysis.

4	/# of categories
0.3129 0.1741 0.1601 0.353	/proportions
1	/background category
mcmod.dbg	/name of debugging file
tpxyz2.bgr	/output file for 3D model
det2.bgr	/output file for determinant
0.01 0.01 0.01	/determinant extent for 3D model
400.0 400.0 10	/dx, dy, dz for 3D model
tpxm2.eas	/x-direction output file
200 400.0	/x-direction: # lags, spacing
2	/option 2: build model based on empirical tp at some lag
PST3mSubTph.dat	/empirical tp functions, horizontal
3	/generate model based on lag 3 (1200 m)
tpym2.eas	/y-direction, output file
190 400.0	/y-direction: # lags, spacing
2	/1=r, 2=d, 3=etp, 4= etf, 5=i, 6=p, 7=f
PST3mSubTph.dat	/empirical tp functions, horizontal
3	/generate model based on lag 3 (1200 m)
tpzm2.eas	/z-direction output file
55 10	/z-direction: # lags, spacing
2	/option 2: build model based on empirical tp at some lag
PST3mSubTpv.dat	/ empirical tp functions, vertical
3	/generate model based on lag 3 (9.144 m)

TSIM

The TSIM code in TPROGS is used to generate 3D conditional stochastic simulations.

4	/number of categories
0.2823 0.1918 0.1324 0.3935	/proportions
PST3mSub2.grd	/output file
2	/output format: 1=binary, 2=ascii
1	/debugging level
tsim.dbg	/debugging file
1212759	/seed
1	/number of simulations
260200 200 400.0	/xmin (grid node), nx, xsiz
4106200 190 400.0	/ymin (grid node), ny, ysiz
640 55 10.0	/zmin (grid node), nz, zsiz
1 4	/min, max # of conditioning data
1	/ibasis: 0=cov, 1=tp
0.001	/wratio
tpxyz2.bgr	/trans. prob. model file
det2.bgr	/determinant file
PST3mSubSlim.dat	/input data file
0. 0.	/azimuths: coord, true
0. 0.	/dip: coord, true
junkaz.bgr	/azimuth int*1 file
junkdip.bgr	/dip int*1 file
4 0.00001 -1	/maxit; tol; -1=no dcl, 1=lag1
0.4	/limit by determinant
7.5	/width of legend (inches)
Empirical	/label for file 1 data
Model	/label for file 2 data

KTB3D

The KTB3D function in GSLIB is used for 3D kriging.

START OF PARAMETERS:

PST3mSubSlim.dat	/data file
1 2 0 3	/column for x, y, z and variable
-1.0e21 1.0e21	/data trimming limits
ktb3d.out	/output file of kriged results
1	/debugging level: 0, 1, 2, 3
ktb3d.dbg	/output file for debugging
200 260200 400.0	/nx, xmin, xsiz
190 4106200 400.0	/ny, ymin, ysiz
1 0 1	/nz, zmin, zsiz
1 1 1	/x, y and z block discretiztion
2 16	/min, max data for kriging
0	/max per octant (0 = not used)
800.	/maximum search radius
0.0 0.0 0.0 1.0 1.0	/search: ang1, 2, 3, anis1, 2
0 2.302	/1=use sk with mean, 0=ok+drift
0 0 0 0 0 0 0 0 0	/drift: x, y, z, xx, yy, zz, xy, xz, zy
0	/0, variable; 1, estimate trend
0	/1, then consider external drift
5	/column number in original data
extdrift.dat	/gridded file with drift variable
4	/column number in gridded file
1 0.0	/nst, nugget effect
2 10.0 0.8	/it, aa, cc: 1=sph, 2=exp, 3=gau
0.0 0.0 0.0 1.0 1.0	/ang1, ang2, ang3, anis1, anis2

SGSIM

The SGSIM program in GSLIB uses sequential Gaussian simulation to generate multiple realizations of the mean permeable fraction distribution.

START OF PARAMETERS:

```
PST3mSubSlim.dat                    /data file
1   2   0   3    0                  /column for x, y, z, variable, dcls weight
-1.0e21   1.0e21                    /data trimming limits
0                                   /0=transform the data, 1=do not transform
sgsim.trn                           /output transformation table
0.0    30.0                         /zmin, zmax (tail extrapolation)
1        0.0                        /lower tail option, parameter
4        2.0                        / upper tail option, parameter
sgsim.out                           /output file for simulation
1                                   / debugging level:  0, 1, 2, 3
sgsim.dbg                           / output file for debugging
112063                              /random number seed
1                                   /kriging type (0=SK, 1=OK)
1                                   /number of simulations
200   260200     400.0              /nx,xmin,xsiz
190   4106200   400.0               /ny,xmin,xsiz
1       0             1             /nz,xmin,xsiz
1                                   /0=two part search, 1=data nodes
0                                   /max per octant (0 -> not used)
800.0                               /maximum search radius
0.0   0.0   0.0   1.0   1.0         /sang1, sang2, sang3, sanis1, 2
0       8                           /min, max data for simulation
8                                   /# of simulated nodes to use
1        0.0                        /nst, nugget effect
2  10.0  0.8                        /it, aa, cc, 1=sph, 2=exp, 3=gau
0.0    0.0   0.0   1.0   1.0              /ang1, ang2, ang3, anis1, anis2
```

Appendix D: Example Drilling Logs

Appendix D contains examples of KGS sample logs and corresponding drillers' logs generated for 4 project test holes drilled in southwestern Kansas. The appendix also contains an example of a water well completion (WWC-5) log. The examples are not intended to represent all subsurface conditions in the study area.

Project test holes drilled in southwest Kansas.
Lithologic Data

Well name: Morton County test hole #1
ID: 667801
Well location: SW Sec. 36, T. 31 S., R. 40 W.
Easting, m: 267829
Northing, m: 4132155
Depth of test hole, m: 146
Land surface elevation, m: 996
Log type: KGS sample log

Lithology	From (m)	To (m)
Moderate yellowish brown clayey silt, calcareous silt	0	3
Dark yellowish brown fine sandy silt, clayey silt, calcrete	3	9
Moderate yellowish brown fine-coarse sand w/ sandy silt, clay, and calcrete	9	12
Grayish orange silt w/ fine to coarse sand and pea gravel	12	18
Light brown fine to med sandy silt w/ calcite-cemented sand & calcrete	18	24
Moderate yellowish brown sandy silt w/ sand, pea gravel, clay, and calcrete	24	30
Yellowish brown sandy silt, fine-coarse sand, calcareous silt, rig chatter	30	40
Sandy silt w/ clay, fine to coarse sand, iron- and calcite-cemented sand	40	43
Grayish sandy silt w/ clay, fine to medium sand, calcareous silt, cemented sand	43	46
Silt and fine to medium sand	46	52
Grayish orange sandy silt, fine to coarse sand, calcareous silt, cemented sand	52	55
Fine to coarse sand & silt, coarse sand and gravel, some silty mudballs	55	61
Fine to coarse sand with cemented sand and Mn oxide; rig chatter	61	64
Fine to coarse siltstone, iron-cemented ss, Mn oxde, calcareous silt	64	73
Fine to medium sand w/ mud balls, silt, cemented sand, and Mn oxide	73	76
Silty to sandy clay with calcite-cemented sand	76	79
Light olive gray silty shale, sandstone, and calcareous silt	79	82
Clayey silt, fine sand with olive black shale; organic odor	82	85
Olive black shale and silty shale; rig chatter	85	104
Olive black shale with sandstone and dark yellowish brown siltstone	104	107
Medium dark gray shale, greenish-gray siltstone, and sandstone	107	110
Fine to medium-grained sandstone, gray shale, and black shale	110	111
Greenish gray siltstone, very fine-grained sandstone w/ dark gray shale	111	119
Dark yellowish orange siltstone, dark gray shale, ferruginous sandstone	119	125
Grayish orange pink siltstone, gray shale, limestone, ferruginous ss	125	128
Dark gray shale, grayish pink siltstone, ferruginous sandstone	128	143
Grayish orange siltstone, dark gray shale, iron- and calcite-cemented ss	143	146

Well name: Morton County test hole #1
ID: 6678010
Well location: SW Sec. 36, T. 31 S., R. 40 W.
Easting, m: 267829
Northing, m: 4132155
Depth of test hole, m: 146
Land surface elevation, m: 996
Log type: Driller's log

Lithology	From (m)	To (m)
Surface	0	1
Brown sandy clay	1	3
Brown clay (firm)	3	12
Sand fine to med course, small to few med gravel	12	18
Cemented sand limerock	18	23
Red cemented sand, limerock	23	24
Sand, fine to med course, small gravel, brown and white rock (reddish tint)	24	27
Fine sand (cemented)	27	29
Brown clay, limerock, silty sands	29	37
Cemented sand	37	43
White clay	43	44
Brown clay, cemented sand	44	48
White-brown clay, cemented sand	48	55
Sand fine to med course, small to med gravel, brown and white rock	55	74
Cemented in places (used some water)	74	77
Gray-white soapstone, few sandstone	77	82
Sandstone (look like sand) (loose lost circ mixed bran)	82	84
Grayish orange siltstone with cemented sand, strong organic odor	84	85
Olive black shale with some silty shale	85	104
Shale, few sandstone (hard)	104	107
Soapstone, limestone (very hard 352-354)	107	108
Soapstone, some sandstone (tight)	108	119
Yellow soapstone, some sandstone (tight)	119	123
Yellow soapstone, few sandstone	123	146

Well name: Morton County test hole #2
ID: 667802
Well location: SW Sec. 36, T. 31 S., R. 40 W.
Easting, m: 267582
Northing, m: 4131910
Depth of test hole, m: 128
Land surface elevation, m: 990
Log type: KGS sample log

Lithology	From (m)	To (m)
Topsoil; dark brown silt	0	3
Brown sandy silt	3	7
Medium to coarse sand with brown sandy silt, calcrete, and pea gravel	7	9
Fine to coarse sand with light gray siltstone and calcrete, drill chatter	9	12
Gravel and fine to medium sand with calcite-cemented sand	12	15
Medium to coarse sand with gravel, calcareous sandy silt, and calcrete	15	15
Brown sandy silt with coarse sand and calcrete; rig chatter	15	21
Brownish gray sandy silt, sand, and calcrete; rig chatter	21	24
Red sandy silt, caliche with coarse sand	24	30
Light brown sandy silt with calcrete, some drill chatter	30	37
Tan silt and medium to coarse sand with pea gravel	37	42
Fine to coarse sand; rig chatter	42	43
Fine to coarse sand and calcite-cemented sand	43	49
Fine to medium sand with coarse sand grains intermixed; rig chatter	49	52
Fine to medium sand and cemented sand with coarse sand; rig chatter	52	57.9
Tan sandy silt with medium sand; rig chatter	57.9	58.2
Fine to coarse sand with pea gravel	58.2	61
Coarse sand and small to medium gravel; rig chatter	61	64
Medium to coarse sand and gravel with cemented silt; rig chatter	64	67
Fine to coarse sand and gravel; rig chatter	67	76
Very fine to fine light tan sand with medium to coarse sand	76	84
Olive black silty shale	84	91
Olive black shale with iron-cemented very fine sand	91	98
Olive black shale; rig chatter	98	104
Olive black silty shale with greenish-gray siltstone; rig chatter	104	113
Dark yellowish orange siltstone	113	119
Yellowish orange and tan siltstone	119	125
Dark red shale	125	128

Well name: Morton County test hole #2
ID: 667802
Well location: SW Sec. 36, T. 31 S., R. 40 W.
Easting, m: 267582
Northing, m: 4131910
Depth of test hole, m: 128
Land surface elevation, m: 990
Log type: Driller's log

Lithology	From (m)	To (m)
Top soil	0	1
Brown sandy clay w/ few sand, sand beds	1	12
Sand fine to med course small gravel	12	17
Brown clay	17	23
Brown sandy clay w/ few small sand strips	23	31
Sand fine to med w/ few small clay stringers	31	34
Brown sandy clay	34	42
Sand fine to med course w/ few clay ledges	42	46
Sand fine to med w/ few clay stringers	46	55
Blue and brown clay	55	58
Sand fine to med course small med gravel - used water	58	74
Fine white sand w/ couple gray soap stone strips - used water	74	83
Gray soap stone and sand stone	83	84
Shale and sand stone strips	84	105
Sand stone and few soapstone	105	108
Sand stone w/ couple soap stone strips	108	113
Yellow and gray soap stone	113	118
Sand stone and soapstone	118	123
Yellow soap stone	123	125
Red bed	125	128

Well name: Seward County test hole #2
ID: 739202
Well location: SW Sec. 35, T. 32 S., R. 34 W.
Easting, m: 323087
Northing, m: 4121136
Depth of test hole, m: 125
Land surface elevation, m: 883
Log type: KGS sample log

Lithology	From (m)	To (m)
Top soil, light yellowish brown silty clay	0	3
Silty clay, with calcite-cemented sand, Mn oxide film, rig chatter	3	6
Fine to coarse sand	6	12
Light tan to yellowish orange clay	12	15
Yellowish orange clay, some Mn oxide coating	15	18
Yellowish orange silty clay with some calcite-cemented sand	18	23
Fine to coarse sand and small gravel with some tan silty clay	23	24
Fine to coarse sand, tan silty clay and small gravel	24	27
Orange silty to sandy clay with fine-grained sand	27	34
Yellowish orange silty clay	34	37
Sandy to silty clay w/ fine to med sand, pedogenic carbonate	37	40
Light brown sandy silt, yellowish orange silty clay, caliche	40	43
Yellowish orange sandy silt, fine to med sand	43	49
Fine to medium silty sand	49	52
Dark tan sandy silt, tan silty clay, fine to coarse sand	52	55
Some chatter, fine to coarse silty sand, some gravel and clay	55	61
Fine to coarse sand with silty clay	61	64
Rig chatter, fine to coarse sand w/ silt, small gravel	64	72
Yellowish brown silty to sandy clay with fine to coarse sand	72	73
Fine to coarse sand, small to medium gravel	73	85
Fine to coarse sand, silt, silty clay, rig chatter	85	91
Yellowish brown clayey silt, fine sand	91	98
Yellowish orange silt with some sandy silt and cemented silt	98	101
Reddish brown sandy silt	101	107
Dark reddish brown clayey silt, yellowish brown silt	107	119
Yellowish brown clay, silty clay with fine silty sand	119	125

Well name: Seward County test hole #2
ID: 739202
Well location: SW Sec. 35, T. 32 S., R. 34 W.
Easting, m: 323087
Northing, m: 4121136
Depth of test hole, m: 125
Land surface elevation, m: 883
Log type: Driller's log

Lithology	From (m)	To (m)
Top soil – sandy -	0	0.6
Fine sand	0.6	1.2
Brown sandy clay	1.2	6
Sand fine some med	6	11
Brown sandy clay	11	19
Red sandy clay w/ some sand strips	19	21
Brown sandy clay	21	23
Sand fine to med course some small couple med and large gravel	23	26
Brown sandy clay	26	37
Brown sandy clay w/ few small sand strips	37	45
Sand fine to med course	45	50
Brown and light blue sandy clay w/ some sand strips	50	55
Sand fine to med course small gravel w/ couple clay stringers	55	72
Brown sandy clay	72	73
Sand fine to med course small gravel	73	86
Sand fine to med w/ some clay stringers	86	91
Brown clay	91	104
Fine sand w/ some clay ledges	104	113
Brown sandy clay w/ couple sand beds	113	118
Gray clay	118	124
Red bed	124	128

Well name: Seward County test hole #3
ID: 739203
Well location: SW Sec. 35, T. 32 S., R. 34 W.
Easting, m: 323648
Northing, m: 4121201
Depth of test hole, m: 146
Land surface elevation, m: 878
Log type: KGS sample log

Lithology	From (m)	To (m)
Top soil, sandy silt, calcite-cemented sand	0	3
Orange-brown clayey, sandy silt, calcite-cemented sand	3	5
Rig chatter, fine sand	5	9
Fine sand, some cemented sand, some clay	9	12
Orange-tan clay	12	15
Orange yellowish brown silty clay	15	24
Orange yellowish brown clayey silt, fine to coarse sand	24	27
Sandy silt w/ clay, fine to coarse sand	27	30
Fine to coarse sand with silt, rig chatter	30	37
Fine to coarse sand, rounded to sub-rounded quartz	37	40
Sandy clay, clay	40	43
Orange reddish brown silty clay, sandy clay	43	49
Orange yellowish brown clay with silt	49	52
Orange red brown sandy silt, orange yellow brown silty clay	52	55
Silty fine to coarse sand with reddish brown sandy clay	55	58
Fine to coarse sand with orange tan sandy silt, small gravel	58	64
Fine to coarse sand, sandy silt, small gravel, sandy clay	64	76
Fine to coarse sand, silty sand, small gravel, rig chatter	76	94
Orange yellowish-brown clay	94	95
Fine to coarse sand, small gravel with silt, rig chatter	95	98
Fine to coarse sand, silty clay, reddish clay, small gravel	98	101
Fine to coarse sand, orange yellowish brown clayey silt	101	107
Sandy clay	107	109
Fine to coarse sand	109	110
Reddish brown clayey to sandy silt, fine to large gravel, clay	110	113
Orange gray clay, fine sandy silt	113	116
Orange yellow brown sandy clay, gray-blue clay, fine sand	116	125
Silty sand, fine to coarse sand, yellowish brown sandy clay	125	128
Red-brown silt, yellow-brown clayey silt, fine to coarse silt	128	131
Fine to coarse silty sand, yellow-brown sandy clay	131	134
Light reddish brown clay, sandy gray blue clay, sandy silt	134	143
Orange-brown sandy silt, silty fine to medium sand, clay	143	146

Well name: Seward County test hole #3
ID: 739203
Well location: SW Sec. 35, T. 32 S., R. 34 W.
Easting, m: 323648
Northing, m: 4121201
Depth of test hole, m: 146
Land surface elevation, m: 878
Log type: Driller's log

Lithology	From (m)	To (m)
Top soil – lime rock and sand	0	1
Brown sandy clay w/ lime rock ledges	1	5
Fine sand	5	9
Brown sandy clay w/ couple sand beds	9	27
Fine sand – couple cemented ledges	27	37
Sand fine to med course few small gravel	37	40
Brown clay	40	56
Sand fine to med course few small gravel	56	69
Sand fine to med course	69	71
Brown and light blue sandy clay	71	94
Sand fine to med	94	95
Brown sandy clay w/ some sand strip and sand beds	95	101
Fine sand w/ some clay ledges	101	104
Brown and light blue sandy clay	104	109
Sand fine to med	109	110
Brown sandy clay w/ some sand strips and sand beds	110	116
Fine sand w/ some clay ledges	116	120
Sand fine to med few course strips	120	128
Fine sand	128	133
Brown sandy clay	133	137
Fine sand	137	143
Brown sandy clay	143	145
Red bed	145	146

Water Well Completion (WWC-5) record

WATER WELL RECORD Form WWC-5 KSA 82a-1212

1 LOCATION OF WATER WELL: County: HASKELL | Fraction: ¼ ¼ NE ¼ | Section Number: 2 | Township Number: T 27 S | Range Number: R 31 E(W)

Distance and direction from nearest town or city street address of well if located within city?

2 WATER WELL OWNER: Clayton Unruh
RR#, St. Address, Box # : Rt1 Box 36B
City, State, ZIP Code : Copeland, Ks 67837
Board of Agriculture, Division of Water Resources
Application Number:

3 LOCATE WELL'S LOCATION WITH AN "X" IN SECTION BOX: N, NW, NE, W, E, SW, SE, S; 1 Mile

4 DEPTH OF COMPLETED WELL. 250 ft. ELEVATION:
Depth(s) Groundwater Encountered 1. 162 ft. 2. ft. 3. ft.
WELL'S STATIC WATER LEVEL 162 ft. below land surface measured on mo/day/yr 2-27-98
Pump test data: Well water was 195 ft. after 1 hours pumping 400 gpm
Est. Yield 500 gpm: Well water was 207 ft. after 2 hours pumping 510 gpm
Bore Hole Diameter 28 in. to 250 ft., and in. to ft.
WELL WATER TO BE USED AS: 1 Domestic 3 Feedlot 5 Public water supply 6 Oil field water supply 8 Air conditioning 9 Dewatering 11 Injection well 12 Other (Specify below)
(2) Irrigation 4 Industrial 7 Lawn and garden only 10 Observation well
Was a chemical/bacteriological sample submitted to Department? Yes.....No.....; If yes, mo/day/yr sample was submitted
Water Well Disinfected? (Yes) No

5 TYPE OF BLANK CASING USED: 1 Steel 3 RMP (SR) 5 Wrought iron 6 Asbestos-Cement 7 Fiberglass 8 Concrete tile 9 Other (specify below)
(2) PVC 4 ABS
CASING JOINTS: Glued X Clamped Welded Threaded
Blank casing diameter 16 in. to 170 ft., Dia in. to ft., Dia in. to ft.
Casing height above land surface 12 in., weight 19.75 lbs./ft. Wall thickness or gauge No. sdr 26
TYPE OF SCREEN OR PERFORATION MATERIAL: 1 Steel 2 Brass 3 Stainless steel 4 Galvanized steel 5 Fiberglass 6 Concrete tile (7) PVC 8 RMP (SR) 9 ABS 10 Asbestos-cement 11 Other (specify) 12 None used (open hole)
SCREEN OR PERFORATION OPENINGS ARE: 1 Continuous slot (3) Mill slot 2 Louvered shutter 4 Key punched 5 Gauzed wrapped 6 Wire wrapped 7 Torch cut 8 Saw cut 9 Drilled holes 10 Other (specify) 11 None (open hole)
SCREEN-PERFORATED INTERVALS: From 170 ft. to 250 ft., From ft. to ft.
From ft. to ft., From ft. to ft.
GRAVEL PACK INTERVALS: From 20 ft. to 250 ft., From ft. to ft.
From ft. to ft., From ft. to ft.

6 GROUT MATERIAL: 1 Neat cement 2 Cement grout (3) Bentonite 4 Other
Grout Intervals: From 0 ft. to 20 ft., From ft. to ft., From ft. to ft.
What is the nearest source of possible contamination: 1 Septic tank 2 Sewer lines 3 Watertight sewer lines 4 Lateral lines 5 Cess pool 6 Seepage pit 7 Pit privy 8 Sewage lagoon 9 Feedyard 10 Livestock pens 11 Fuel storage (12) Fertilizer storage 13 Insecticide storage (14) Abandoned water well 15 Oil well/Gas well 16 Other (specify below)
Direction from well? How many feet?

FROM	TO	LITHOLOGIC LOG	FROM	TO	LITHOLOGIC LOG
0	5	top soil			
5	10	clay			
10	40	sand			
40	91	sand & gravel with clay stripe			
91	110	sand & gravel with rock			
110	115	sand & clay			
115	125	sand & gravel with rock			
125	128	lime rock			
128	190	med gravel			
190	195	clay			
195	205	course sand			
205	220	sandy clay			
220	230	clay			
230	240	fine sand			
240	332	sandy clay			

7 CONTRACTOR'S OR LANDOWNER'S CERTIFICATION: This water well was (1) constructed, (2) reconstructed, or (3) plugged under my jurisdiction and was completed on (mo/day/year) 2-27-98 and this record is true to the best of my knowledge and belief. Kansas Water Well Contractor's License No. 367 This Water Well Record was completed on (mo/day/yr) 3-30-98
under the business name of Grosch Irrigation by (signature)

INSTRUCTIONS: Use typewriter or ball point pen. *PLEASE PRESS FIRMLY* and *PRINT* clearly. Please fill in blanks, underline or circle the correct answers. Send top three copies to Kansas Department of Health and Environment, Bureau of Water Protection, Topeka, Kansas 66620-7320, Telephone: 913-862-9360. Send one to WATER WELL OWNER and retain one for your records.

Appendix E: Interpolation Errors

This section summarizes the residual errors of practical saturated thickness (PST) estimates generated from various gridding and interpolation techniques.

Table E-1. Selected 2D Interpolation Results

ID	Grid name	Interpolation method	Details	R	RMS	MAE
1	pre_001	closest point	high fidelity, smoothing=1	0.98	3.917	1.039
2	pre_002	closest point		0.96	5.756	1.144
3	pre_003	Inverse distance	weighting exp=2, 8 pts, sector-based searching=15%, 15°, 24 sectors	0.96	6.469	3.87
4	pre_004	Inverse distance	weighting exponent=1.5, 3 points	0.96	6.075	3.511
5	pre_005	Inverse distance	weighting exponent = 2, 8 points	0.96	5.844	3.18
6	pre_006	Inverse distance	weighting exponent = 2, 3 points	0.97	5.457	2.667
7	pre_007	Directional weighting	direction: 45°, strength: moderate	0.95	6.977	3.711
8	pre_008	Directional weighting	direction: 9°, strength: moderate	0.94	7.419	3.983
9	pre_009	Directional weighting	direction: 90°, strength: moderate	0.94	7.47	4.02
10	pre_010	Directional weighting	direction: 9°, strength: strong	0.93	7.843	4.273
11	pre_011	Directional weighting	direction: 9°, strength: weak	0.94	7.05	3.645
12	pre_012	Directional weighting	direction: 351°, strength: moderate	0.93	7.574	4.013
13	pre_013	Triangulation	high fidelity, smoothing x1	0.98	3.917	1.039
14	pre_015	Inverse distance	weighting exp=2, 3 pts, decluster = 400	0.96	6.155	3.04
15	pre_016	Inverse distance	w exp=2, 3 pts, decluster=400, 1st order poly	0.96	6.155	3.04
16	pre_017	Closest point	decluster = 400	0.96	6.215	1.417
17	pre_018	Closest point	high fidelity, smoothing x1	0.98	3.917	1.039
18	pre_019	Closest point	high fidelity, smoothing x2	0.98	3.917	1.039
19	pre_020	Closest point	high fidelity, smoothing x1, density x2	0.98	3.917	1.039
20	pre_021	Triangulation	high fidelity, smoothing x1	0.98	3.917	1.039
21	pre_022	Kriging	decluster, resolution = 400	0.94	7.292	4.424
22	pre_023	Kriging	high fidelity, smoothing x 1	0.98	3.917	1.039
23	pre_024	Kriging	high fidelity, smooth x1, 1st order poly	0.98	3.917	1.039
24	pre_025	Multiple Linear Regression	anisotropy 1.5x, 10 pts, dist=100, h.f., smooth x1	0.98	3.917	1.039

Appendix F: Hydraulic Head Residuals

This section summarizes the residual errors of hydraulic head in the ground-water flow simulation.

Table F-1. Selected results of the homogeneous flow simulation

Run	Conductance (m^2/d)	K_x (m/d)	RMS (m)	MAE (m)	R	Total In (m^3)	Recharge (m^3)	ZBud Discrepancy (%)
M1	20	24.4	7.43	5.80	0.994	397910	130460	0%
M2	3	24.7	5.24	3.98	0.995	6767	184	-0.11%
M3	15	8	6.71	5.21	0.995	126650	32520	0%
M4	15	14	7.31	5.73	0.994	176210	12280	0.01%
M5	15	0.65	4.94	3.79	0.995	10861	0	-0.04%
M6	5	8	6.22	4.85	0.995	113540	12393	0.01%
M7	20	24.7	7.78	6.25	0.993	372480	73213	-0.01%
M8	20	24.7	8.51	6.62	0.992	111030	53810	0.01%

Table F-2. Selected results of the heterogeneous flow simulation

Run	Conductance (m^2/d)	K (m/d)	RMS (m)	MAE (m)	R	Total In (m3)	Recharge (m3)	ZBud Discrepancy (%)
T1	50	Indicator Variables	4.86	3.92	0.99	25805	5007	0%
T2	5	Indicator Variables	6.14	4.95	0.99	45772	493	0.01%
T3	5	Indicator Variables	5.37	3.95	0.99	21777	5007	0%
T4	0.815	Indicator Variables	7.79	6.20	0.99	2772	327	0.05%
T5	50	Average K, Closest Point	7.94	6.86	0.98	161170	5007	0%
T6	50	Log K (Gutentag et al., 1981)	8.40	6.82	0.99	109560	1.55E-12	0.02%
T7	50	1st K	8.63	7.15	0.99	110360	5007	0.01%
T8	50	Indicator Variables	5.36	3.99	0.99	21777	5007	0.01%